Light-Controlled Rheology of Living Suspensions of *Chlamydomonas reinhardtii*

Author:
Constance Timmermans

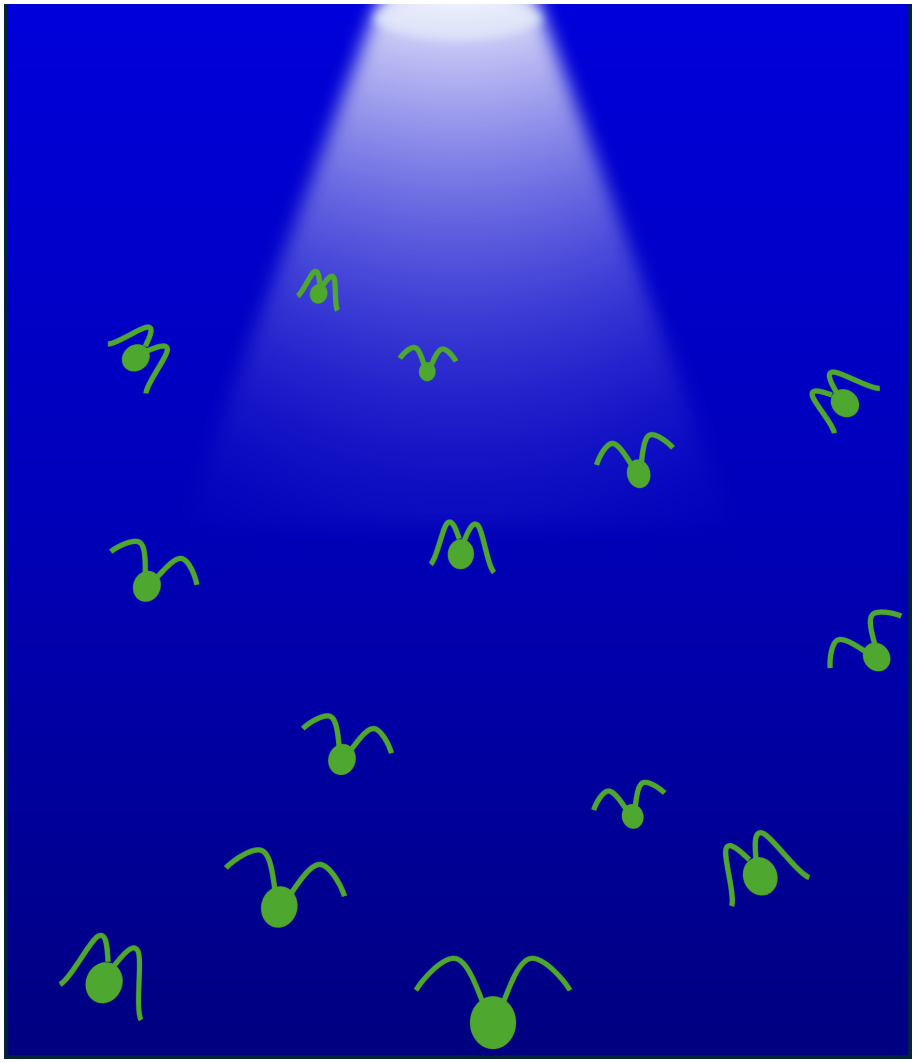

Supervisors:
D.S.W. Tam
Sowmya Kumar

Process & Energy Department
Delft University of Technology
The Netherlands

August 2024

Light-controlled rheology of living suspensions of *Chlamydomonas reinhardtii*

by

Constance Timmermans

to obtain the degree of Master of Science
at Delft University of Technology
to be defended publicly on August 12, 2024

Student number:	4785312	
Thesis duration:	September, 2023 - August, 2024	
Thesis committee:	Dr. D.S.W. Tam	TU Delft, supervisor
	Dr. A. Laskari	TU Delft, committee member
	Sowmya Kumar	TU Delft, daily supervisor

TU Delft Delft University of Technology

Abstract

The presence of living organisms in a fluid can affect a fluid's properties. Organisms propel themselves through the fluid using specialised organelles that generate propulsion. This propulsion creates disturbances in the fluid, leading to variations in its properties. The overarching research question is: "Can the properties of a fluid be modified with biologically active suspensions?". Organisms respond to their environment for survival and thereby induce intriguing patterns which enhance flows. By using their natural instincts to react to external stimuli, fluid systems could generate flows or intrinsically modify their properties, which can be controlled by a user's own will. It is thought that the local orientation of the organism influences the viscosity in a shear flow, because of the added stress induced by the activity of the organisms. This research investigates the influence of the orientation of the stress induced by the green alga *Chlamydomonas reinhardtii* on the viscosity using light-controlled rheology. This is done through two research questions: "Is it possible to modulate the swimming orientation of the green algae using a light source?", followed by the question: "Can we thereby control the viscosity of the algal sample?".

Phototaxis is the natural response of the algae to swim in the direction of light and was the main asset used to control the swimming orientation. The first research question was explored through three-dimensional microscopy. Images were acquired from algae controlled by light entering at a specific angle of 45°. The second research question combined light-control with a rheometer that imposed an external shear flow. The rheometer measures the viscosity of light-controlled algae using an on-and-off light cycle.

Through the three-dimensional imaging, the position and velocity vectors of each particle was found and converted into the relevant spherical coordinates which in turn could present the trajectories of the organisms. These were found to be swimming at the targeted angle at sufficient light intensity. The second experiment however showed ambiguous viscosity responses that had to be quantified using power analysis. The quantification of the data showed possibility of a viscosity change as a result of the reorientation towards light.

The first experiment showed the possibility to control the orientation of the algae using phototaxis and thus positively answering the first research question. The second research question cannot be answered taking strong conclusions. The quantification of the data showed possibility of a viscosity change as a result of the reorientation towards light.

Acknowledgement

I would like to express my deepest gratitude to my professor, Daniel Tam, for providing me with this project and for his invaluable insights throughout the process. The topic, which involved elements of biology - a notable divergence from the usual mechanical topics - was both intellectually stimulating and rewarding. His guidance has been instrumental in shaping the direction and outcomes of my research.

I extend my heartfelt thanks to my daily supervisor, Sowmya Kumar, for her unwavering support and assistance. Her input was crucial in obtaining meaningful results, and her help with both major and minor aspects of the project was indispensable. Both my professor and my daily supervisor pushed me to become the best version of myself, continually challenging me to improve my engineering approach, thereby enhancing the quality of my work.

I also wish to thank Professor Angeliki Laskari for her valuable role as a member of my thesis committee.

Finally, I am profoundly grateful to my family for their constant support and encouragement during this thesis. Their belief in me has been a source of strength and motivation.

Contents

List of Figures

Chapter 1

Introduction

Fluids are central to industrial and biological processes and their rheological properties determine the flow dynamics. The rheology of a fluid strongly depends on the nature of the fluid and on the particles or molecules which are suspended or disturbed in the fluid. Suspending solid particles in a fluid are known to increase the viscosity and dissolving long polymeric chains alters the viscoelastic properties of the fluid.

The functionalities of a fluid can be enhanced and tailored for specific applications by designing it such that its rheology can be modified and controlled by an external field. The development of smart fluids, which are fluids that can be controlled using external triggers, presents a transformative opportunity in fluid dynamics and material science. Examples of such smart fluids include magnetorheological and electrorheological fluids, which are actuated by external magnetic or electric fields and have found application in clutches, vibration dampers, braking systems and in batteries [10].

In recent years, a new class of suspensions known as active suspensions has emerged and garnered significant interest. Active fluids are fluids in which self-propelling particles are present. In these suspensions, the particles are moving independently within the continuous liquid phase. Recent work on active fluids is found on the emergence of a collective motion occurring between self-propelling particles and developed the influences this collective behaviour has on the rheological properties of the fluid. The natural response of active particles on their environment makes active suspension well-suited for designing new smart fluids.

The focus of this thesis is to explore the possibility of creating a smart fluid, using living biological organisms, where the viscosity can be modified as desired. The green algae *Chlamydomonas reinhardtii* are utilized to develop a light-responsive active fluid. Phototaxis refers to organisms moving toward light, propelled by flagella that disturb the surrounding fluid during movement. Theoretical models suggest that this changes the viscosity. While mathematical models attempt to predict the effects of organism activity on the surrounding fluid, they often lack experimental validation. This research aims to help filling the gap between theory and real-world applications and contribute with experimental evidence. Rheology is the study of deformation and flow of matter [4]. It allows for the analysis of the effects on the viscosity of the active fluid. As part of this research, the objective is to design and create a system that includes phototaxis during rheology, followed by performing light-controlled rheology on algae suspensions and analyse the changes in viscosity.

Following from the previously mentioned objectives, the general research question for this thesis is:

Can the properties of a fluid be modified with biological active suspensions?

The structure of the paper starts with this introduction in which more background is given on the topic of smart fluids, followed by more information on the biological concepts

and finishing with the main research questions. In chapter 2, a theoretical framework on the fluid dynamics will be elaborated. Chapter 3 provides an overview of the laboratory procedure of the biological organisms used during the entirety of the research. Two experiments cover this research and are discussed in chapters 4 and 5. Their research methodology, including the experimental setup and the procedure followed, and the results are provided in detail together within the chapters. The data collected is analysed simultaneously for clarity. Each chapter includes a discussion on the experiment. The paper terminates with the conclusion in chapter 6.

1.1 Smart Fluid Systems

Smart fluids are fluids whose properties can be manipulated by applying an external stimulus on the system. Through impulses such as electric or magnetic fields, light, temperature, etc., it is possible to impose an external field and generate flows. Smart fluids are also called liquid engineered systems or autonomous liquids. While modifying the rheological properties of a fluid, a fluid can be controlled with the use of external cues. This paragraph will dive deeper into the creation of smart fluids that are currently developed.

Although this area of research is an intersection of biotechnology, materials science and engineering, the design of an internally driven flow is yet unexplored [14]. The most reported smart fluids are magnetorheological and electrorheological fluids. These fluids contain solid particles, that align with the imposed magnetic and electric field, respectively, which in turn creates a chain between neighbouring particles that trigger a change in viscosity [33]. These have been studies in the late 40's and have since then been applied in various technologies, such as brake systems, clutches and in batteries [10]. Other rheological properties that might be modified are the elasticity of liquids. This is achieved by thermoreversible gels [6]. Through changing temperatures, a liquid mixture experiences a phase transition to a gel. All these property changes a rise from within the liquid and are caused by the fluid's composition.

Compositions of fluids can also be modified using living organisms. As the organisms can respond to their environment for reasons of survival, they develop collective motions that result in complex dynamics inside the fluid. A natural phenomenon is the formation of biofilms, where organisms collect and adhere to each other, creating a dynamic colony able to adapt to environmental stresses such as nutrient deficiency and predators [27]. The motility of organisms has been established in applications to drive objects such as gears [26][39] serving as actuators [20] or to develop cargo delivery and transport [13][21]. The collective behaviour of organisms has also been used to generate fluid flows as a new pumping system [13][19]. Research has attempted to mimic the biological organisms, because of their interesting properties. Microrobots have emerged and have served various purposes in research [1]. Controlling self-propelling particles, even when human-made, remains challenging. Through the use of an external impulse such as light, pattern flows could be created, forming vortices, shear and mixing fields [14], with the ability to switch from one pattern to another by varying the light-control or even maintain two different flows simultaneously.

Smart fluids are valuable due to their creative implementation in technology, particularly in biomedical applications [11]. These fluids, composed of self-propelling particles, offer significant advantages in small-scale systems and exhibit a high degree of autonomy. Optimizing these systems and and mastering their control is essential for their successful application in technology. These systems remain built from individual particles that require nutrition and energy, making it more difficult to program flows in the bulk [14].

1.2 Biological Background

In biology, organisms are classified into eukaryotes and prokaryotes. Prokaryotes are a domain of organisms which lack a nucleus, whereas eukaryotes do have a nucleus. Algae belong to the simplest group of eukaryotes called protists. Together with many other organisms, such as fungi, plants, and animals, protists form a kingdom of eukaryotes. Fluids are omnipresent to every form of life and play a role in biological processes.

The biological fluid dynamics involved in this literature review is the locomotion of eukaryotes. Locomotion refers to how organisms move in their surrounding fluid. Eukaryotes achieve swimming motion by propelling themselves using slender organelles called flagella. The flexible flagella of the eukaryotes are similar to muscle fibres and generate flows and propulsive forces through their actuation. A flagellum is constructed as follows: the axoneme serves as the internal structure, surrounded by long polymeric filaments or microtubule doublets arranged in a 9+2 configuration. The filaments slide past each other, resulting in bending waves of the flagellum. The actuation of the filaments is driven by ATP-powered molecular motors. Dynein is a type of protein that converts the chemical energy stored in ATP into kinetic energy. Protists have varying numbers of flagella that they utilize in diverse ways to move themselves forward. The function of the flagella is mainly to create propulsion in a fluid, which makes them swim towards a preferred location. Their swimming orientation is influenced by external factors, including nutrients and photosynthesis. The requirement for the latter is the presence of light, which will be discussed next.

1.2.1 Phototaxis and Light Properties

Phototaxis is the locomotion of an organism towards or away from a light source. The relevant light properties are discussed in this section. These include intensity, light spectrum and light direction. In the case of phototaxis, microorganisms swim towards or away from light, denoted by positive or negative phototaxis, respectively. Light has an impact on their growth, capacity to perform photosynthesis and is beneficial for survival in ecological environments [36]. This is the reason why selecting the right light conditions during experimental research is crucial to control organisms with phototaxis.

The first important property discussed is the light intensity, which is the main feature for controlling the behaviour of various microswimmers [36][16]. The swimming direction of cells depends on the intensity. Cells move towards a critical light intensity I_c optimal for their eyespot. Excessive intensity can damage the photoreceptor [16]. Light intensity is influenced by obstacles encountered along the path. This causes light absorption or light reflection, shading or scattering of light [16]. In dense suspensions, light intensity decreases with depth because of scattering due to the suspended particles.

The position of the light source relative to the organism influences phototaxis as well. The eyespot of the green algae *Chlamydomonas reinhardtii* is on the side of its body, such as illustrated in figure 1.1. The cells will position themselves in a way to achieve the light more effectively [44]. The algae are also gravitactic. Their centre of mass is not in the centre of the body, but slightly closer to the bottom of the body. Therefore, a torque is induced on the body, which makes the cell swim in an upward direction [44]. A greater light intensity is needed for downward phototaxis [44]. In order to help the cells, their body works as a convex lens [31], directing the light entering their body towards the eyespot.

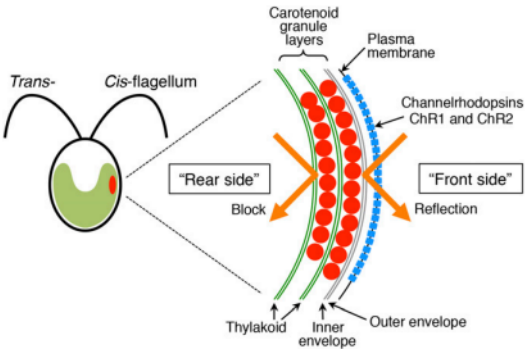

Figure 1.1: Illustration of the position of the eyespot of the *Chlamydomonas reinhardtii* and how it is built. It contains carotenoid (red) layers and photoreceptor proteins (blue). The carotenoid layers act as a barrier to block the light coming from the inside of the cell.

The colour of the light source is another light property that must be chosen correctly. The algae *Chlamydomonas reinhardtii* are sensitive to wavelengths in a range of $370 - 550nm$ [16][44], corresponding to blue and green light. Unlike blue light, the wavelengths covering red light do not affect the algae and are therefore not effective for phototaxis [44][18].

1.3 Research Question

This chapter discussed the motivation behind this research. In this thesis, two separate questions are investigated and answered through two sets of experiments. First, an important concept in the theory is the biased preferential swimming orientation of organisms. In a laboratory frame, the bias can be influenced by using phototaxis to reorient organisms. We take advantage of *Chlamydomonas reinhardtii*, a green alga, which is responsive to light for photosynthesis. The cells rotate to align themselves towards the light source, modifying their swimming orientation.

The first research question is therefore:

1. Is it possible to control and modulate the orientation of *Chlamydomonas reinhardtii*?

As the organisms change their swimming orientation, the hypothesis suggests that this will increase resistance in the fluid, leading to higher viscosity. Therefore, the hypothesis suggests that the viscosity is directly influenced by the orientation, and the following research question is:

2. Is it possible to control the viscosity of the active fluid?

The aim of the thesis is to provide experimental evidence for the hypothesis by fixing the orientation of algae using phototaxis. The viscosity of the active fluid will be measured with a rheometer, which imposes an external shear flow on the active fluid.

Chapter 2

Theoretical Framework

2.1 Fluid Dynamics Equations and Concepts

In this chapter, the important micro-hydrodynamic concepts are introduced, necessary to understand the dynamics of a microorganism's locomotion. First, the governing Stokes equations are derived, followed by the dynamics of the motion of an individual organism, including how their flagella result in the motion of the organisms. The induced stress system is explained physically following from the flow singularities. Subsequently, these dynamics are taken to rheology and elaborate on the influence of the orientation.

2.1.1 Governing Equations: Stokes Flow

Considering a swimmer of size L propelling at speed U in a fluid with density ρ and dynamic viscosity μ. Two timescales dominate this problem [22]. First, the timescale $t_1 = L/U$ for a perturbation to be advected along the swimmer. Second, the timescale $t_2 = \rho L^2/\mu$ for a perturbation to be dissipated by viscosity. The ratio of the timescales forms the dimensionless Reynolds number:

$$Re = \rho LU/\mu$$

An important property of the Reynolds number is to analyse the dominant force of the fluid dynamics problem. The Reynolds number can be viewed as the ratio of the inertial forces and the viscous forces. For Reynolds numbers much smaller than unity, the viscous forces dominate. The organism studied is the *Chlamydomonas reinhardtii*, which is a single-cell green alga with two flagella. From experimental data, the length scale L is known to be $\sim 10\mu m$ and the mean swimming velocity $v_s = 78\mu m/s$ [2]. The density of the active fluid with *Chlamydomonas reinhardtii* suspensions is close to the density of water, because the body of the biflagellate organism consists mostly of water [25]. This results in a Reynolds number of approximately $Re \approx 10^{-3}$, with $\mu/\rho \approx 10^{-6}$ [22].

Consider the organism prescribed above with length scale L, varying its body shape in time with an average frequency ω. Its varying body shape comes from the fluctuating flagella which results in locomotion. The deformation of organisms leads to a flow in the surrounding fluid in which stresses arise. Using some basic fluid dynamics, the conservation of momentum can be written by Cauchy's incompressible momentum equations

$$\rho\frac{\partial u}{\partial t} + \rho(u\cdot\nabla)u = \nabla\cdot\sigma, \qquad \nabla\cdot u = 0 \tag{2.1}$$

in which σ is the stress tensor. Newtonian fluids are characterized by constant dynamic viscosity and the stress tensor is given by $\sigma = -pI + 2\mu E$, with the dynamic pressure p, the dynamic viscosity μ, the identity matrix I and the rate of strain tensor $E = (\nabla u + \nabla u^T)/2$. From this, equation 2.1 becomes the incompressible Navier-Stokes equations

$$\rho\frac{\partial u}{\partial t} + \rho(u\cdot\nabla)u = -\nabla p + \mu\nabla^2 u, \qquad \nabla\cdot u = 0 \tag{2.2}$$

Because viscous forces are dominant, one can simplify the Navier-Stokes equations into a non-dimensional form using normalized variables time $t^* = t\omega$, velocity $u^* = u/U$, gradient $\nabla^* = L\nabla$ and pressure at high viscosity $p^* = pL/(\mu U)$. Replacing the variables in the Navier-Stokes gives the following form

$$Re_\omega \frac{\partial u}{\partial t} + Re(u \cdot \nabla)u = -\nabla p + \mu \nabla^2 u \tag{2.3}$$

with

$$Re_\omega = \frac{\rho L^2 \omega}{\mu}, \qquad Re = \frac{\rho L U}{\mu} \tag{2.4}$$

The Reynolds number, previously discussed, appears in the dimensionless Navier-Stokes equations. Because the Reynolds number is small, some terms vanish and the equations can be simplified to:

$$\nabla p = \mu \nabla^2 u, \qquad \nabla \cdot u = 0 \tag{2.5}$$

which represent the Stokes equations. These provide a unique solution corresponding to the flow of swimming organisms. Organisms require an effective mechanism of propulsion to move in a viscous fluid. This is achieved by thin organelles, called flagella. To move in a Stokes flow, the flagella employ the form of a propagating wave. The remainder of this section contains the theoretical concepts, which result from the governing equations, on how an organism's individual motion results in an induced stress system around the particle and how this affects the rheological properties of a fluid.

2.1.2 Flow Singularities and Induced Stress System

The form of flagella beating dynamics leads to flow disturbances that contribute to the total stress in the fluid. By obtaining the flow field through the Stokes equations, two flow singularities appear: the Stokeslet and the source dipole. The Stokeslet represents a point force acting at a specific location in the fluid, which is the simplest way of representing the fluid system. However, the forces applied by the organism are not a single net force, but a force dipole, see figure 2.1. This arises from the drag and thrust of the organism. The force dipole is a dominant term in the flow surrounding the microorganism [22][5][37]. It is decomposed into a symmetric and antisymmetric part, named the stresslet and rotlet, respectively [5]. The rotlet is a flow resulting from an external net torque on the fluid. The stresslet is a flow induced by the microswimmer's flagella beating. The stresslet is defined by a stress tensor $\mathbf{S}$ that accounts for the extra stress generated by the flagella and is of the following form:

$$\mathbf{S} = \Sigma_s(\mathbf{pp} - \frac{\mathbf{I}}{3}) \tag{2.6}$$

where $\mathbf{p}$ is the orientation vector of the organism [22][23]. Because the stress tensor originates from the force induced by the flagella, F, and because of its symmetry, it follows:

$$S_{11} = -S_{22} = -2aF \quad S_{33} = 0 \tag{2.7}$$

Based on this stress, the organisms can be categorized into two groups, see figure 2.2. Organisms that pull the fluid in their longitudinal axis and push the fluid away from the sides are called pullers showing the stress induced of a puller, such as the green alga *Chlamydomonas reinhardtii*. They create contractile flows [37], see figure 2.2b. In contrast, if the fluid is pushed away in the longitudinal axis of the body and withdrawn from the sides, the organism is called a pusher, e.g. *Escherichia coli*. In this case, the organisms induce extensile flows [37], see figure 2.2a. This stresslet is induced by all motile organisms in the active fluid, and they all collectively contribute to stresses induced in the fluid. The higher the volume fraction of the algae suspensions, the more the effect of the additional stresslet influences the viscosity [30][35][46]. The stresslet is a leading-order term that approximates the flagellar disturbances in the far-field [22].

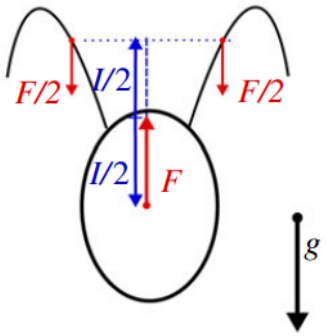

Figure 2.1: Force dipole created by the flagella of the green alga. [16]

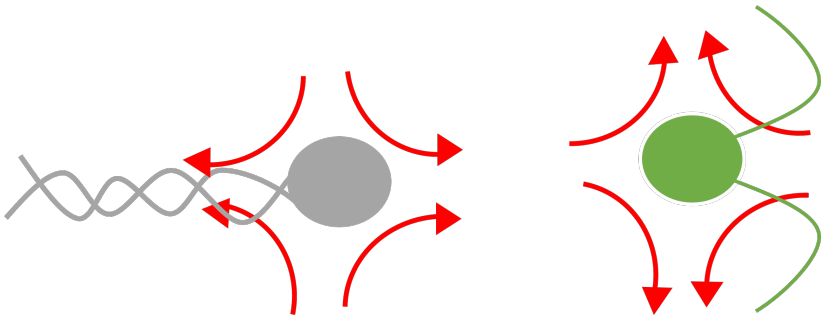

(a) Stresslet created by pusher. (b) Stresslet created by puller.

Figure 2.2: Stresslets created by flagellar propulsion divide organisms in pushers or pullers.

2.1.3 Rheology of Active Fluids and the Role of Orientation

By applying an external force, the fluid responds to the conditions to which it is exposed and the fluid properties can be analysed. During rheology experiments, a fluid sample is confined between two parallel plates. The upper boundary rotates around its central axis, while the lower is stationary. When the upper plate rotates, it drags the fluid along with it due to the fluid's viscosity. This creates a velocity gradient in the fluid, known as shear flow, represented by the step-like schematic in figure 2.3. The rotational speed determines the shear rate. In this way an external shear flow is imposed on the fluid in a controlled manner, and the torque exerted on the top plate is measured with sensors. From torque measurements, the stress exerted by the fluid can be inferred and viscosity is measured. Viscosity is a measure of a fluid's resistance to deformation and flow and can be calculated using the relationship between shear stress and shear rate:

$$\eta_{eff} = \frac{\sigma}{\dot{\gamma}} \tag{2.8}$$

with σ the shear stress and $\dot{\gamma}$ the shear rate. The shear flow is a superposition of a translation, a rotation and a straining motion at 45° [37][22], see figure 2.4.

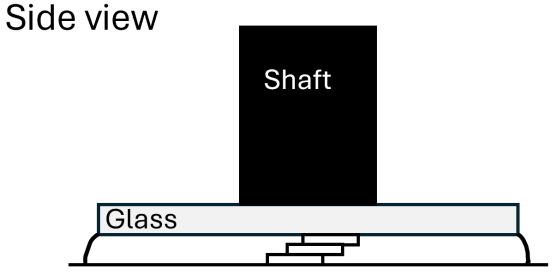

Figure 2.3: Side view of the external imposed shear flow by the rheometer.

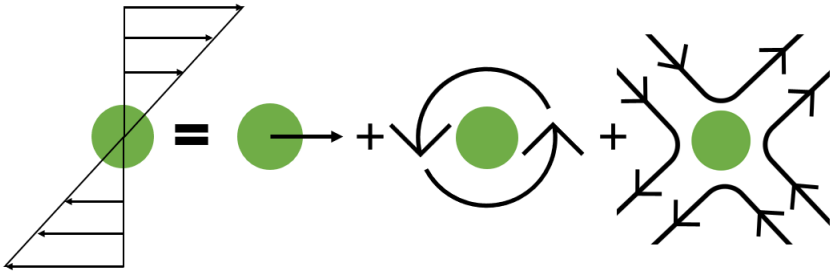

Figure 2.4: Superposition of flow singularities of a passive particle in a shear flow. From left to right it includes the shear flow equal to the superposition of a translation, a solid body rotation and a straining flow field.

Adding solid and passive particles in a fluid increases the viscosity [15]. This is a phenomenon dependent on the concentration of the passive particles and distinguished in a dilute or concentrated regime [15]. Passive particles induce a flow field, or disturbance field, in the presence of an external flow due to the no-slip boundary condition at the surface of the particle [37]. When immersing them in a shear flow, the particles can translate and rotate with the suspending fluid, but because they are rigid, they cannot stretch with the fluid. By resisting the local straining flow, they impose a stress on the fluid, called the passive stress, which leads to an increase in the viscosity at macroscale [37].

This theory was further extended for particles that are not spherical, but elongated [5]. The particle's orientation and movement are primarily influenced by the shear flow's velocity gradient and align themselves with respect to the imposed flow. The orientation of the particle is determined by the aspect ratio of its geometry and is described by Jeffery's orbits [17]. Interactions between neighbouring elongated particles result in the alignment of the particles in a nematic order in which they align their longitudinal axes [22][37]. Most of the particle's time is spend in the extensional part of the shear flow. This mean orientation enhances the net effect of the passive stress on the viscosity [37].

When that particle is also motile, such as in the case of living organisms, the stress system induced by the flagella - the stresslet described in the previous paragraph - is linearly added to the stress and is called the active stress. Its origin lies in the flagellar beating and the stress induced by the rigid particle [37]. This active stress is assumed to be the reason for observed rheological changes in the active fluid [37][40][35][47][28]. It is thought that the orientation of the active stresslet can superimpose the local straining motion and thus enhance the flow [41]. Active stresses are generated by the flagella. Therefore, the orientation of the active stresslet with respect to the flow depends on the swimming direction. When organisms swim along the extensional or compressional axis of the straining motion in the shear flow, there is a maximum contribution to the overall stresses in the fluid.

The effect of the active stress of a puller is studied here. When the extensional axis of the active stresslet aligns the extensional aixs of the straining motion, the viscosity is suggested to decrease as it enhances the flow. Conversely, when the contractile axis of the active stresslet is aligned with the extensional axis of the straining motion in the shear flow, it resists the fluid flow and therefore increases the viscosity. Figure 2.5 illustrates the orientation of the stresslet with respect to the straining motion of the shear flow. The effect of the stresslet on the viscosity is bigger with increasing cell concentrations [35].

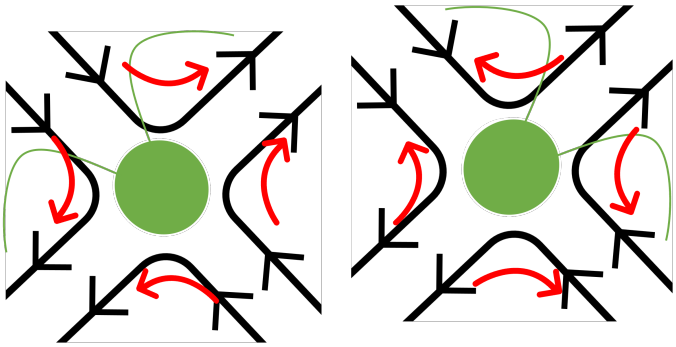

(a) Viscosity decrease (b) Viscosity increase

Figure 2.5: The orientation of the active stress is thought to impact the viscosity according to the resistance or enhancement to the external imposed shear flow. The black arrows represent the straining motion of the shear flow and the red arrows represent the induced active stresslet of the organism.

Chapter 3

Standard Procedure of Green Algae

The studied organism is the *Chlamydomonas reinhardtii*, which is a single-cell green alga with two flagella that propel the organism through the fluid. This alga is commonly used for scientific research purposes, because of the ease to culture the cell. This chapter details the laboratory procedure used for this study.

3.1 Biological Organisms: green algae - *Chlamydomonas reinhardtii*

The first topic covers the main element of this research: the culture of algae suspensions used for the experiments. This chapter will talk about the growth of the *Chlamydomonas reinhardtii* and will clarify the step-by-step plan to grow a culture. The laboratory procedure is an embedded process that needs to be carried out carefully, because working with microbiological agents requires a standard sterile procedure to eliminate contamination and to guarantee a successful and healthy culture.

C. reinhardtii need an energy source for growth. As a photosynthetic microorganism, the algae can grow under light together with an inorganic carbon source, such as carbon dioxide. The organism can also grow without light by using an organic carbon source, such as acetate [38]. Here, a light source is used for the growth of *C. reinhardtii*. The algae are stored in a glass test tube within a solid medium containing nutrients. In order to imitate natural living conditions, the test tube containing the algae are placed into a closed box with a light bulb inside, following a day-night cycle, corresponding to 14 hours light and 10 hours dark by switching the light on and off. Light guarantees cell growth and division, where photosynthesis creates biomass and energy. In the dark cycle, the cells produce DNA, which is used for their successive mitotic divisions during the night [9]. Figure 3.1 illustrates this process. Mitosis is the cellular division process that leads to the equal distribution of genetic material, producing daughter cells that are genetically identical.

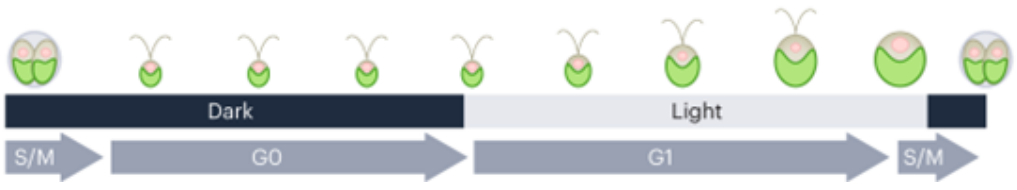

Figure 3.1: Growth of *C. reinhardtii* cells and division illustrated. Light cycle stands for growth and ends with DNA production. Night cycle provides mitotic division. [9]

Inscriptions on the test tube indicate the algal strain CC125 and two dates corre-

sponding to the previous culture from which the current was extracted and the second date the day that the culture was started. From this test tube, a new culture is created on a Tris-based medium. This can be Tris (Tris(hydroxymethyl)aminomethane) or TAP (Tris-Acetate-Phosphate) and is specified in the experimental procedure. Tris-based solutions provide nutrients for the algae and are a growth medium supporting culture growth to high concentrations of organisms within the liquid. TAP medium is used when a bigger amount of organisms are required for the experiment, while Tris is a medium used for general purposes and a variety of biological applications. Tris results to lower cell concentrations than TAP. During the rheology experiments, the effect of a collective behaviour is important to capture and therefore higher concentrations are needed. Through the Tris-based medium, the pH of the culture is maintained stable at $pH = 7$. The Tris-based medium is poured into a clean Erlenmeyer flask. Using a loop, the algae are extracted from the solid medium culture to create a new culture in the Erlenmeyer containing the tris-based liquid. This task is performed in sterile conditions to exclude contamination. Once the algae are transferred into the liquid medium, the new culture is placed into a growth box at constant temperature of $25°C$, see figure 3.2. Aeration is provided by blowing filtered air into the solution at approximately one bubble per second. The mass flow of the air is controlled every day. The solution stays in the growth box for five days and can be used afterwards for the experiments. A step-by-step scheme is added in appendix A to provide an overview of all steps and operations by hand in detail.

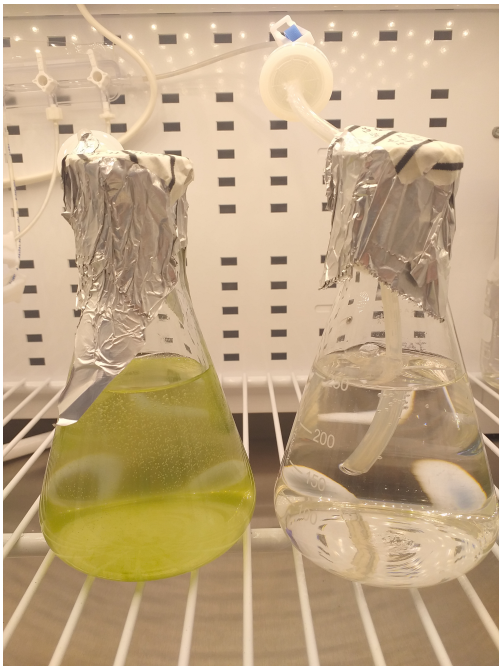

Figure 3.2: Culture of *Chlamydomonas reinhardtii* in Erlenmeyer with aeration.

A higher volume fraction of cells is achieved using a centrifuge, when required for the experiment. A centrifuge uses the principle of sedimentation, which consequently allows for the separation of samples by their density. The first step is to count the initial volume fraction of the culture using a counting chamber, shown in figure 3.3, under the microscope. The cell density is obtained in number of cells per millilitre. The cell count is followed by calculating the amount of times the sample must be centrifuged in order to achieve the desired volume fraction. The algal sample can be diluted in order to minimize the error during counting. The reason behind diluting is that when concentrations are too high, the cells overlap, making it more difficult to count. Cells must be immobilized, or killed, in order to count. Higher volume fractions are obtained using a centrifuge. Instead of waiting for gravity to make the cells settle to the bottom of the flask, a centrifugal force is used to separate particles of different density. This process is followed by removing the

excess TAP medium and gently mixing the remaining sample, without stressing the algae in their new environment as this can cause death or immobility. It is crucial to give the organisms enough time to settle in the liquid after concentrating them.

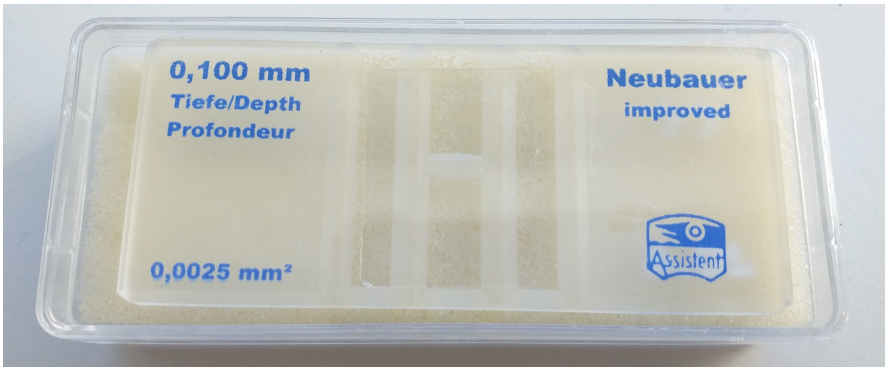

Figure 3.3: Neubauer counting chamber for manual counting of number of cells in a solution.

3.1.1 Two-Dimensional Microscopy

Two-dimensional (2D) microscopy is used to verify the health of the algae within the culture, as well as the concentration. The microscope, Nikon ECLIPSE Ti2, consists of a camera which is connected to a computer. Images and recordings can be obtained through the software pco.camware. By zooming into the cells and recording a range of images, their velocity and flagella beating frequency can be acquired. A velocity of approximately $100\,\mu m/s$ and a flagella beating frequency around $50\,Hz$ are characteristics of a healthy alga. Afterwards, the volume fraction of cells in the liquid solution is found by using a counting chamber under the 2D microscope. The lens used on the microscope is a Nikon ELWD 20x/0.45 and enlarges the image 20 times.

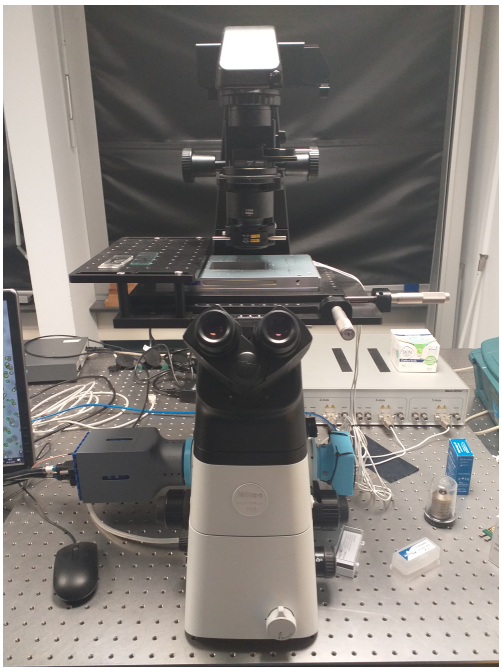

Figure 3.4: 2D microscope Nikon

Chapter 4

Orientation Control Experiment of the Algae *Chlamydomonas reinhardtii*

The first research question is to investigate whether the swimming orientation can be controlled at an angle of 45° by making use of phototaxis. This corresponds to the principle axis of the straining motion of the shear flow. In order to know if the composition of the light incident angle and the light intensity reach the algae suspensions through glass, microscopy will facilitate the observation of the algae's response to the incident light. The three-dimensional imaging provides information on the position of the algae from which we analyse if the trajectory of the algae is oriented towards the light. Confirming the alignment of their trajectory with the required swimming orientation validates if the position of the light source is correct and if the organisms can be controlled through the cell's tactic behaviour.

4.1 Research Methodology

This section will go through the experimental setup that is designed to achieve light-control in a specific orientation, followed by explaining the analysis of the data obtained by 3D imaging.

4.1.1 Experimental Setup for Optical Imaging

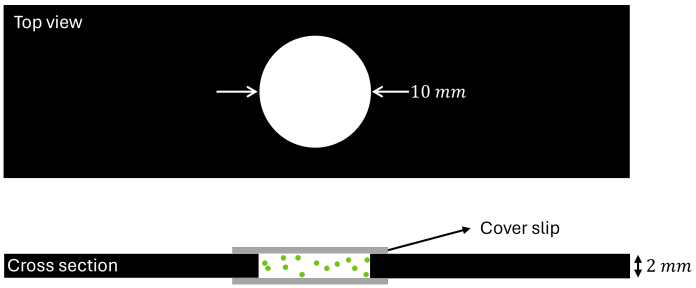

Figure 4.1: Flow cell enclosing the algal sample using two cover slips.

For this experiment, a lower cell concentration is required which is why an algae culture is started in tris. The experiment consists of creating a flow cell carrying the algal sample concentrated at $10^4\, cells/ml$, poured in a $10\, mm$ diameter and $2\, mm$ deep opening enclosed by two thin glass covers glued on top and bottom, as illustrated in figure 4.1. The flow cell is laser cut in a $2\, mm$ thick acrylic plate. The acrylic flow cell is painted in matt black to

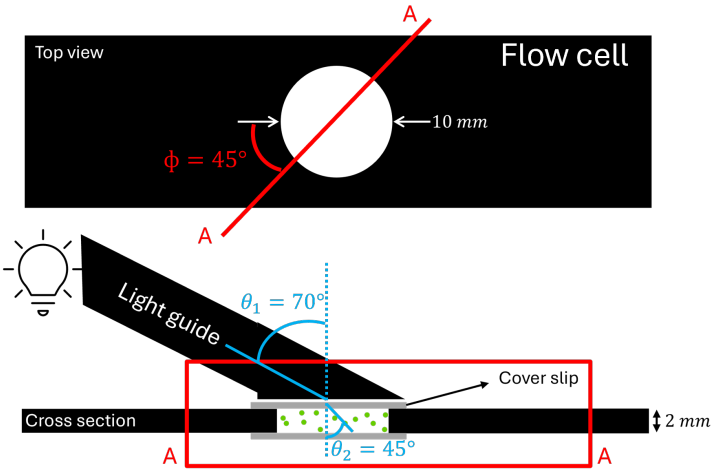

Figure 4.2: Flow cell with light guiding tube positioned at diagonally on top of the flow cell.

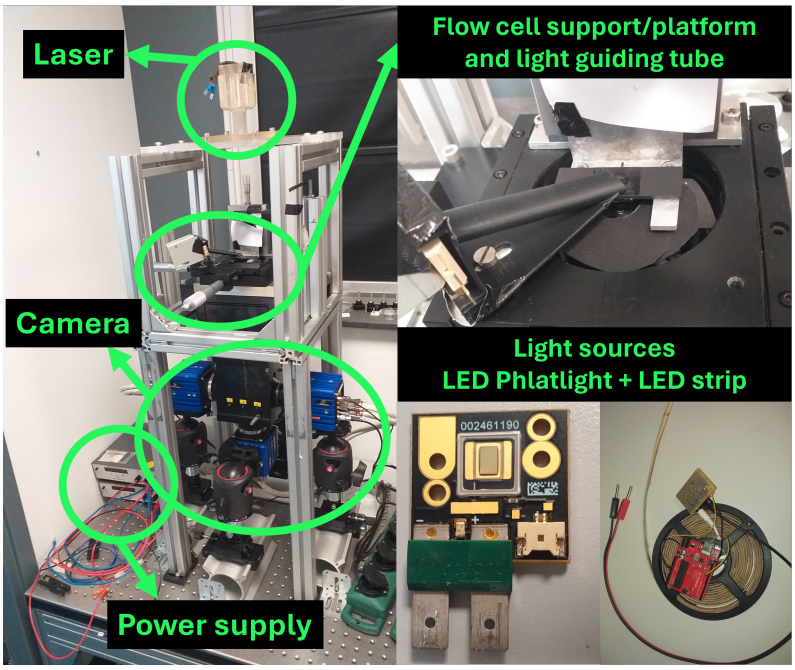

Figure 4.3: 3D microscopy setup consists of four cameras and a laser to obtain an image. A flow cell support serves as a platform for the flow cell and the light guide regulated by a power supply.

prevent reflections within the flow cell and is crucial for this experiment. The black spray paint needs at least 24 hours to dry.

All experiments are performed in a dark room blocking all the light from outside and without any lights in the laboratory switched on, preventing the algae to be able to react to it. Only the light source that is used for phototaxis is switched on. The experiments are performed in the absence of a shear flow. The objective of this experiment is to orient the orientation of the algae at an angle of 45°, to coincide with rheology. The experiment determines whether the light conditions are effective in reorienting the algae at this slope. In order to guide the light into a specific angle into the fluid sample, a light guiding tube is designed through which the light can travel and blocking light coming from any other direction, see figure 4.2. A light source is connected to the black, opaque tube, which is placed on top of the flow cell to illuminate the algal sample, while guiding the light into penetrating the flow cell, as shown in the setup in figure 4.3. The experiment investigates

whether the illumination intensity is sufficient for the algae to perform phototaxis. In addition, the incident angle of the penetrating light is researched as well. Because of the glass cover of the flow cell, light is refracted. This means that the angle of incidence is different than the angle of refraction. The light guiding tube is tilted at a 70° angle with the vertical axis, which using Snell's law corresponds to a refraction angle of 45°. Appendix B explains how the tilt of the light guiding tube is obtained. The tube is designed in Solidworks and 3D printed in black opaque plastic.

Different light sources are tested during the experiment. The light source is fixed on the light guiding tube. The different light sources tested are a cool white LED strip, a green and a white LED Phlatlight. The latter two, from the brand Luminus, are flat light sources capable of emitting a significant amount of light and thus achieving high intensities. Throughout the experiments, the Phlatlights are tested at different intensities that can be obtained by adjusting the power in a power supply. The intensity is measured at the end of the light guiding tube. The light guide system is designed as a template to be used for the setup that will be used on the rheometer and therefore has a length of $8\,cm$, see chapter 5. The geometrical restrictions are taken into account in the design of this experiment to assure that the light properties defined here can be used during rheology. Figure 4.3 shows the setup used for this assessment, together with the light sources. The setup consists of four cameras, a support on which the flow cell rests that also serves as a platform to fix the light guiding tube onto it. From the brand LaVision, DaVis is the software used for image acquisition and processing [7]. In order to create a clear picture, sufficient illumination is required. Therefore, a red laser is added on top and illuminates the entire flow cell, without influencing the behaviour of the algae. Next paragraph will elaborate more on the 3D microscopy.

4.1.2 Three-Dimensional Microscopy and Data Analysis Procedure

Images of the algal sample are obtained using three-dimensional microscopy. An objective lens ensures that the image is visible to the camera by refracting light to form a clear image. The middle of the sample is placed at the focal point of all four cameras, ensuring a good image quality. An objective lens ensures that the image is visible to the camera by refracting the image. It collects light from the sample observed and forms an enlarged image. The magnification of the lens is $M = 1.5$. An additional element is the pinhole, which is part of the microscopy method used, called dark-field microscopy. This technique creates a bright image against a dark background, enhancing the contrast and visibility of fine details or low-contrast particles within the sample. Upon the fixed pinhole, an extra pinhole will be added during the calibration in order to achieve a bigger depth of focus. Consequently, the position and velocity throughout the flow cell are better understood.

The first step is to perform the calibration on the 3D microscope. In this step, using a calibration grid is an essential tool for ensuring the accuracy and reliability of the measurements. A calibration grid is a specialized slide with a grid pattern of dots precisely spaced with 300 microns between each dot and a cross in the middle of the grid. This grid is used to calibrate the magnification of an optical system and determine the size of objects being viewed under the microscope. By comparing the known dimensions of the grid pattern to the size of the image produced by the microscope, the size of the microscopic particles can be measured accurately. The grid is placed on the focal plane, which is one millimetre above the support of the setup, and thus in the middle of the flow cell. Using the cross in the middle of the grid, the four cameras can be aligned with respect to the calibration grid so that all cameras view the same object. Next, the extra pinholes are added, creating a depth of field of $2\,mm$, which corresponds to the depth of the flow cell.

After the calibration, the flow cell is prepared, followed by turning on the red laser, which does not influence the algal activity, but does provide sufficient light to the cameras to reproduce a clear image. Next, the light guiding tube is fixed on the platform and the

LED light source can be fixed to the tube, see figure 4.3. A power supply is needed for both laser and LED light source. Once every item is in place, a recording of the algal activity can be made through the software DaVis. The computer records 2000 frames at 20 frames per second. All three light sources were fixed one by one to the light guiding tube. The LED Phlatlight sources were varied from a lower to higher intensity to observe the intensity at which algae respond and to analyse if their orientation is influenced more strongly. Additionally, the reaction time of the algae is about 3 seconds and was checked during the experiments. The light source was switched on a few seconds after the recording started. It is therefore crucial to capture well the start of the phototactic response, insuring to record the trajectory of the cells completely and quantifying their reaction time using the frame rate. Between each recording, a waiting time of at least five minutes illuminated only by the red laser is imposed for the algae to start swimming again in random directions without stimulating their photoreceptor [42].

After image acquisition, a tracking algorithm is used to convert the image into particle trajectories. Images obtained through DaVis are converted into an $im7$ format before supplying them to the Matlab tracking algorithm, developed by Koen Muller. Through this algorithm, further analysis can be done on the position and velocity of the particles, while they are moving in space. Trajectories are obtained by jointly projecting the positions of each particle of multiple recorded frames. Once the trajectories are reconstructed, the swimming orientation is deduced and compared with the illumination direction.

The data which will be presented are the 3D trajectories and a histogram showing the distribution of the swimming orientation. The trajectories are viewed from the side, so it can be seen immediately whether cells swim in line with the light. The Z-axis is the optical axis along the depth of the flow cell and the light source positioned diagonally on top of the flow cell, which means that the light direction projected onto the XY plane aligns with the $X = Y$ direction. The histogram is a colour map and consists of two parameters defining the direction of the trajectory of the cells. From the spherical coordinate system, figure 4.4, the polar angle θ and the azimuthal angle ϕ best define the trajectory of the particles. The polar angle describes the angle of the trajectory from the Z-axis. The azimuthal angle shows if the trajectory is aligned with the light in the $X = Y$ alignment. A cell swimming towards the light corresponds to $\theta = 45°$, $\phi = 45°$, while a cell swimming away corresponds to $\theta = 45°$, $\phi = 135°$. In order to account for the changing radius in a spherical coordinate system, the variables in the colour map are normalized by $\sin\theta$ to ensure that all variables contribute equally and that the system is not dominated by one variable.

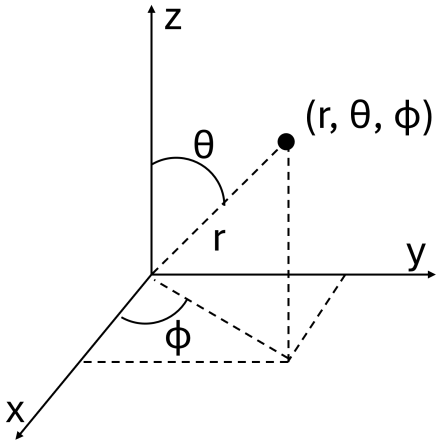

Figure 4.4: Spherical coordinate system, with r the radial distance, θ the polar angle and ϕ the azimuthal angle.

In all the obtained data, the cells perform a helical trajectory in space. Therefore, the

trajectories of the cells were smoothed using a Savitzky-Golay filter over the X, Y and Z positions. In order to extract the locally swimming orientation, the center of the helical path was obtained, representing a straight path, see figure 4.5 to which a bias could be found in the spherical coordinate system.

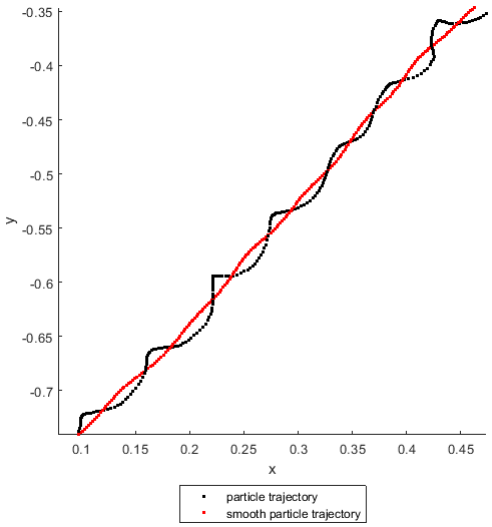

Figure 4.5: Helical trajectories were smoothed through the Savitzky-Golay filter.

Before presenting the results from the different light sources, the data from experiments without any light source is shown in figure 4.6. This provides ab baseline for the random motion of swimming algae that occurs naturally. The trajectories are in random directions, as can be seen through the azimuthal angle, where the distribution is uniform. This means that the cells swim in all directions projected on the XY plane. The polar angle shows that the algae are swimming upwards rather than downwards as they are shifted towards $0°$ with the Z axis. The upward swimming is a result from the gravitaxis of the algae and represents an important factor to consider when analysing the data from the light-controlled experiments. The data processing was performed after the experiments, because it took a considerable amount of time to process and due to IT problems. Consequently, the upward swimming factor was discovered only after performing the experiments. The frame range was reduced in order to analyse the slope of the cells that did not yet achieve the top surface. Additionally, in order to remove reflections or immobile particles, only the cells that swim a minimum distance of $0.25\,mm$ were selected. A total amount between 45 to 60 trajectories were kept as healthy and relevant detected organisms.

4.2 Results of the Orientation Control Experiment of the Algae *Chlamydomonas reinhardtii*

This first experiment consists of finding out whether the swimming orientation of the algae suspensions of *Chlamydomonas reinhardtii* can be controlled with phototaxis. The experimental setup was discussed previously in section 4.1. In short, imaging provides information of the three-dimensional space of the flow cell containing diluted algae. A light guiding tube was placed diagonally on top and reorients the organisms in a specified orientation. The light intensity, light incident angle and the position of the light source are tested.

The light sources were successively connected to the tube. Starting with a white LED strip which emitted $1000\,lm/m$, followed by a green and white LED Phlatlight. The latter two were tested at different intensities. The intensities are measured at the end of the light guiding tube and mentioned with the corresponding light source. The 3D trajectories and

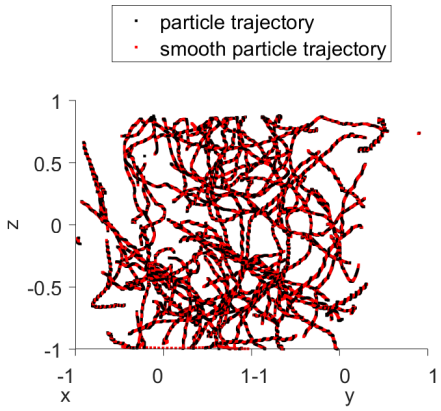

(a) 3D trajectories of algae in a dark environment

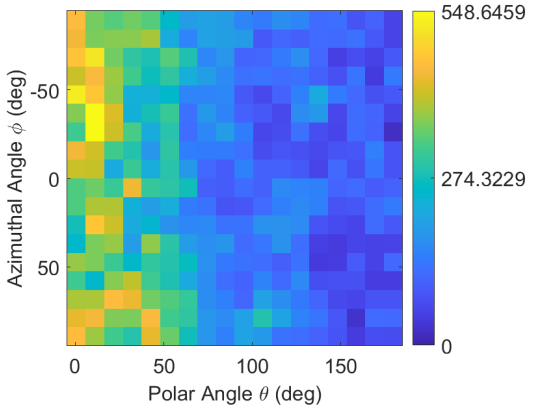

(b) colour map representing the spherical coordinates

Figure 4.6: Results of the 3D imaging of the green algae in a dark environment.

the histogram will be shown in this section for the three different light sources.

4.2.1 White LED strip

The white LED strip was turned on at its maximum intensity, reached at $24\,V$ and a current of $1.5\,A$. The LED strip emits $1000\,lm/m$ and the intensity measured with a light meter at the end of the tube was $5\,\mu mol/mm^2s$. It was not practical to modify the intensity, because of the low emitted intensity. Figure 4.7a shows the 3D trajectories of the cells that follow a path parallel to their neighbouring cells, indicating a phototactic response along the light source. Horizontal trajectories can be seen at the top surface, indicating that the organisms swam at the top surface. The colour map allows to analyse their trajectory in more detail. A peak in the distribution if found in the fourth quadrant of the colour map, representing the majority of tracks at $\theta = 100-150°$, $\phi = 40-60°$, with a larger amount at $\theta = 130-140°$. The meaning of this polar angle indicates a downward orientation of the organisms, meaning that they swim away from the light, called negative phototaxis.

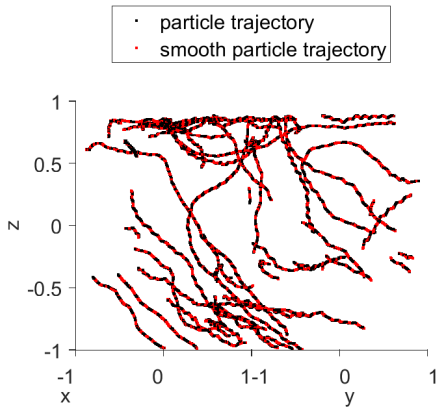

(a) 3D tracks at $24\,V$ equals $5\,\mu mol/mm^2s$

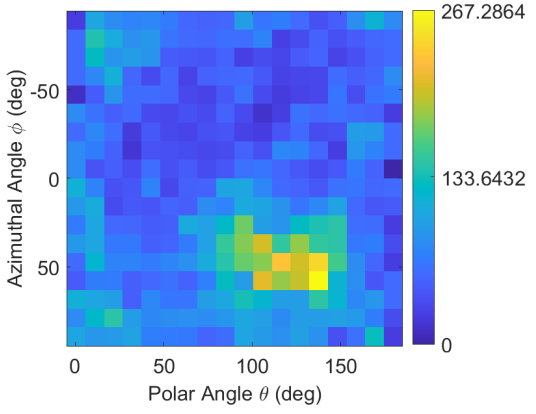

(b) colour map at $24\,V$ equals $5\,\mu mol/mm^2s$

Figure 4.7: Results of the 3D imaging of the green algae under influence of the white LED strip, showing both 3D trajectories and colour map

4.2.2 Green LED Phlatlight

The green LED was tested at $2.6, 2.8, 3, 3.2$ and $3.4\,V$.The intensities measured with the light meter correspond to $0, 2, 9, 33$ and $52\,\mu mol/m^2 s$ respectively, with the intensity measured at the end of the black light guiding tube. An observation made when using the light is that the light source spends its first minute with a slightly lower intensity at the same voltage. As the light source heats up, it reaches higher intensities, which are the ones mentioned here. Precautions must be taken regarding the heat after its warm-up phase. A metal plate is connected to the light source functioning as a thermal conductor. The results of the experiment are placed here in figure 4.8. The different intensities allow for observation of how the trajectories of the algae evolve with increasing intensity. The two lowest intensities show that no phototaxis is happening, as the intensity is too low. At $3\,V$, more cells start to swim towards the light, resulting in a bias at the targeted swimming angle, viewed by a yellow spot at the azimuthal and polar angle of $45°$. The result at $3\,V$ also shows yellow blocks distributed all along the azimuthal angle, meaning that although some cells are react to the light, others do not. The histograms show a bias at a polar angle of $50°$, meaning that the cells are swimming upwards to the light, which is positive phototaxis.

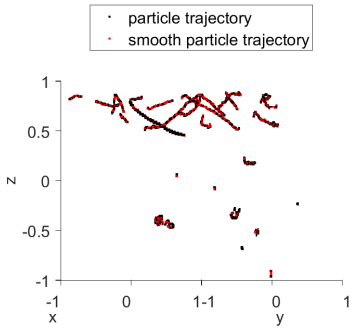

(a) 3D tracks at 2.6V equals 0 $\mu mol/mm^2s$

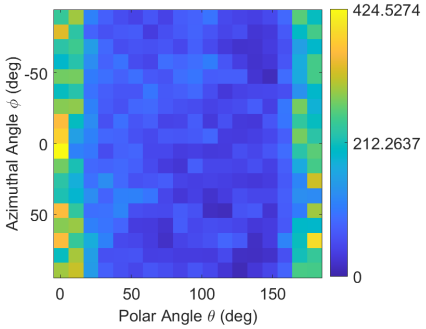

(b) colour map at 2.6 equals 0 $\mu mol/mm^2s$

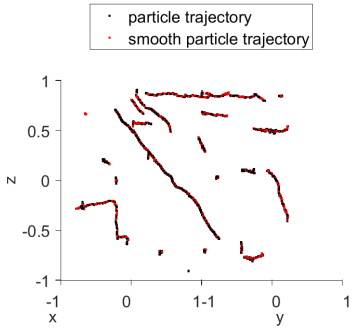

(c) 3D tracks at 2.8V equals 2 $\mu mol/mm^2s$

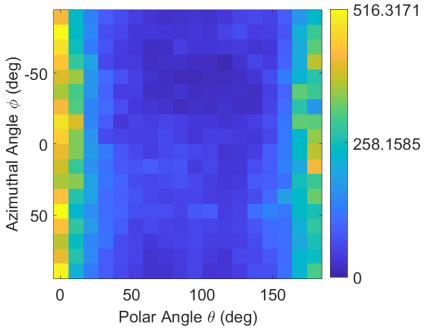

(d) colour map at 2.8V equals 2 $\mu mol/mm^2s$

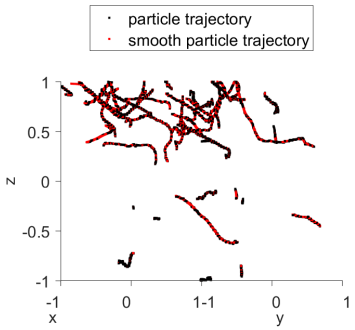

(e) 3D tracks at 3V equals 9 $\mu mol/mm^2s$

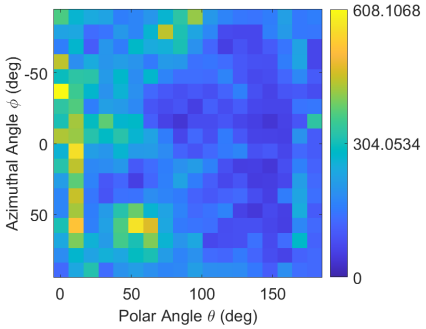

(f) colour map at 3V equals 9 $\mu mol/mm^2s$

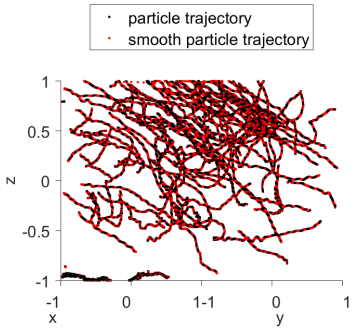

(g) 3D tracks at 3.2V equals 33 $\mu mol/mm^2s$

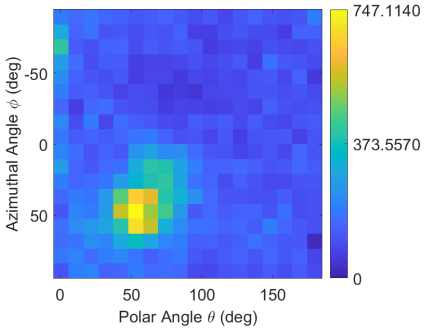

(h) colour map at 3.2V equals 33 $\mu mol/mm^2s$

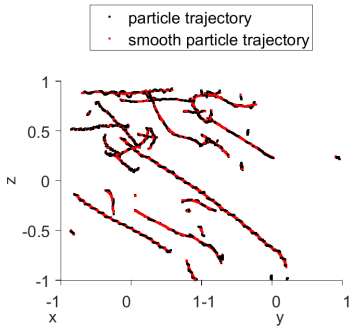

(i) 3D tracks at 3.4V equals 52 $\mu mol/mm^2s$

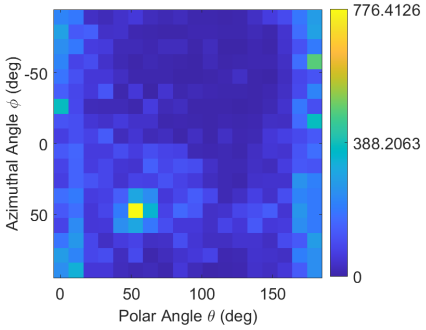

(j) colour map at 3.4V equals 52 $\mu mol/mm^2s$

Figure 4.8: Results of the 3D imaging of the green algae under influence of the green LED Phlatlight, showing both 3D trajectories and colour map

4.2.3 White LED Phlatlight

The white LED was tested at 2.8, 3 and $3.2\,V$. The intensities measured with the light meter correspond to $106, 240$ and $263\,\mu mol/m^2 s$ respectively, with the intensity measured at the end of the black light guiding tube. The last experiment at $3.2\,V$ shows a smaller bias in the desired quadrant, because this experiment includes fewer frames of phototaxis. The measurement was shorter because the light source, a newer model than the previous green LED, heated up much more quickly. However, in the few frames that were captured, the phototactic response was observed positively in the fourth quadrant. For all three intensities, the polar angle is at $50°$, indicating positive phototaxis of organisms swimming up towards the light.

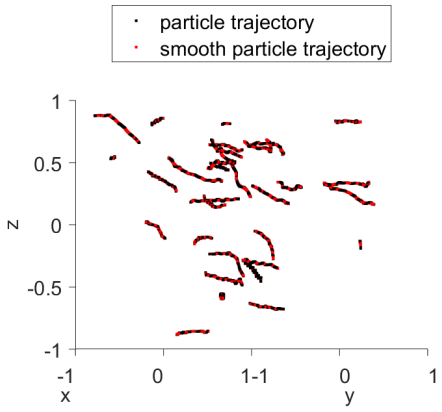

(a) 3D tracks at 2.8V equals 106 $\mu mol/mm^2 s$

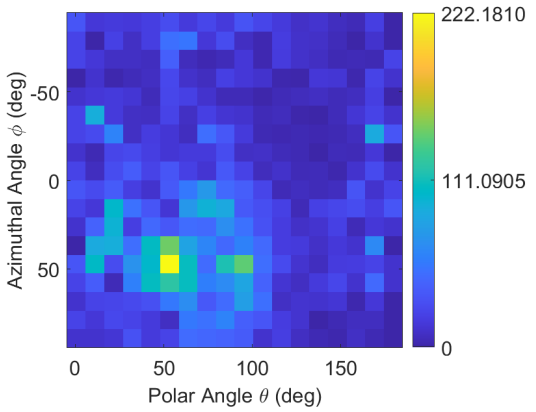

(b) colour map at 2.8V equals 106 $\mu mol/mm^2 s$

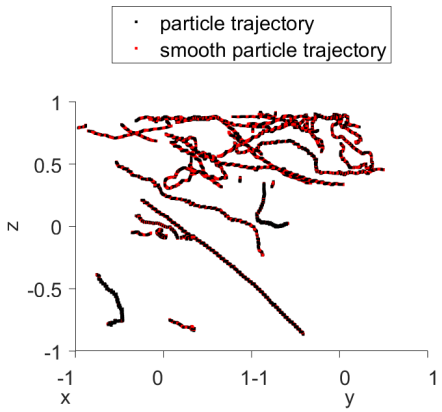

(c) 3D tracks at 3V equals 240 $\mu mol/mm^2 s$

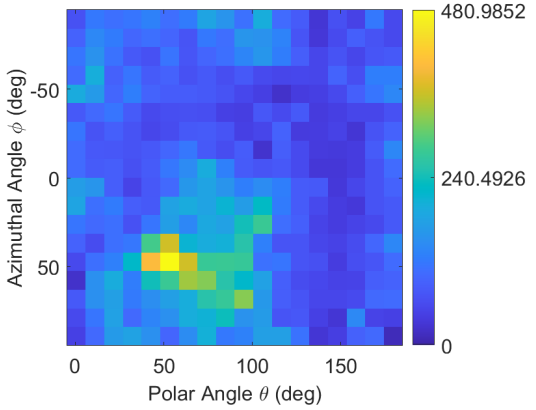

(d) colour map 3V equals 240 $\mu mol/mm^2 s$

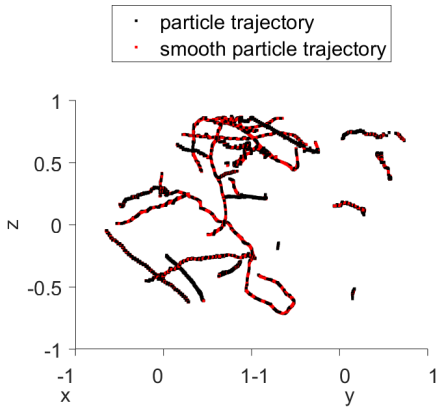

(e) 3D tracks at 3.2V equals 263 $\mu mol/mm^2 s$

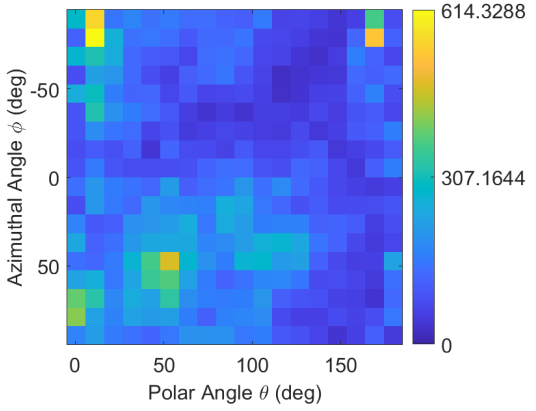

(f) colour map at 3.2V equals 263 $\mu mol/mm^2 s$

Figure 4.9: Results of the 3D imaging of the green algae under influence of the white LED Phlatlight, showing both 3D trajectories and colour map

4.3 Discussion of Orientation Control Experiment of the Algae Suspensions

This chapter aimed to find an answer to the first research question. The topics covered in this chapter were the experimental approach, including the setup designed for the 3D microscopy, followed by the data collection through 3D imaging and its analysis. The orientation of the suspended organisms was characterized by two spherical angles. Through this approach, a colour map was created, indicating the distribution of the swimming orientation. The experimental setup included a tube tilted at a 70° angle with the vertical

axis in order to account for light refraction. The distribution peak was achieved between 45° and 55° for the experiments with sufficient light intensity, meaning that the light reaches the organisms at the target angle. The polar angle shows that for the green and white LED Phlatlight, the organisms perform positive phototaxis, while the white LED strip performs negative phototaxis. Both positive and negative phototaxis are allowed for the targeted trajectory. By looking at different light intensities, it was viewed that the phototactic response was obtained at a minimum intensity of $5\,\mu mol/mm^2s$, although the peaks in the distribution becomes more narrow at increasing light intensities. The experiments highlight the importance of using a black, opaque tube in order to achieve any phototaxis at all. Through the recording, the time reaction to the light source was quantified to 3 seconds, using the frame rate and visually watch the frame at which the organisms reorient. The reaction time is the time when the light source was switched on until the organisms visually reorient themselves and travel towards the light source, calculated by $\frac{frame_{light} - frame_{phototaxis}}{frame\,rate}$. The experiment showed that phototaxis can be used for controlling the orientation of the organisms.

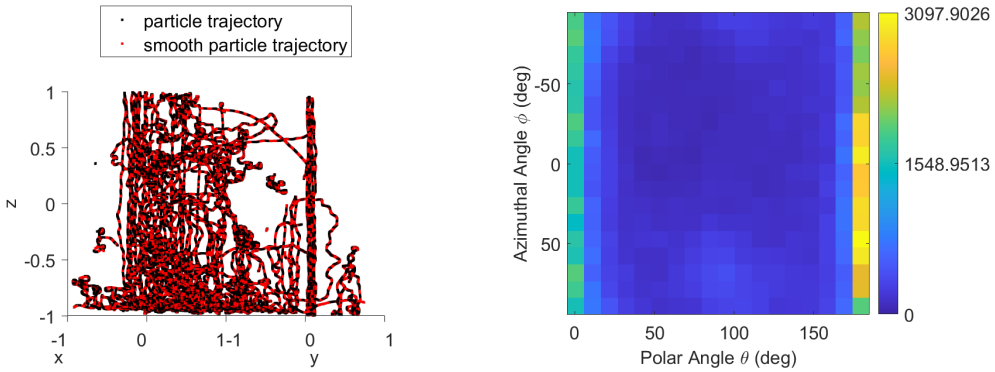

(a) 3D tracks (b) Colour map

Figure 4.10: Results of the 3D imaging of the green algae under influence of a green laser [experiment from Junaid Mehmood].

The light sources used in the experiments were LED lights. These have lower light intensities and are less concentrated than lasers. The light intensity measured from the green laser in the lab was $750\,\mu mol/m^2s$. An experiment was performed by Junaid Mehmood using a green laser. Figure 4.10 shows the results of this experiment on an amount of 190 detected particles. The laser was placed vertically on top of the flow cell. The trajectories show the vertical motion of the organisms. Comparing this result with the results from the LED sources, the green laser shows a more narrow peak of distribution than when using the LED lights. With a laser, the light is more concentrated at the laser spot, while an LED light can illuminate a bigger surface. Therefore, LED lights result in a more homogeneous cell distribution than with a laser where the organisms maximise at the laser spot.

Chapter 5

Rheology of Light-Controlled Algae Suspensions

The focus of this chapter is on the second research question. Here, a suspension of living green algae is sheared continuously, while exposing the suspension principally to a light at 45°. The green algae form an active fluid that is exposed to light during the rheology. The aim is to experimentally study the influence of light-controlled living suspensions on the viscosity in a shear flow. The shear flow is imposed by the rheometer. The particles will be aligned parallel or orthogonal to the straining motion of the shear flow by making use of phototaxis during rheology. The first section provides an overview on the basic principles of the rheometer and the use of additional accessories required for the experiments. There are specific experimental requirements for conducting the rheological studies with biological organisms that cause limitations to the setup. This chapter is a guide through the many parameters influencing the experimental setup.

5.1 Experimental Approach Including a Rheometer

A rheometer is a very sensitive device, measuring the response of a fluid to an external force. It can provide valuable insights on the behaviour and characteristics of different fluids. Rheometers help researchers understand the flow behaviour, viscosity, elasticity, and other important properties of substances. Different types of rheometers exist, divided into two categories: rotational and extensional rheometers. Extensional rheometers apply an extensional stress. Rotational rheometers apply a shear stress or shear strain. The latter is the category used for this thesis. The model of the rheometer used is a Modular Compact Rheometer MCR 302 from Anton Paar.

The rheometer is coupled to a computer which has the software RheoCompass, through which it can be controlled. In order to work with the rheometer, the first step is to initialize the device and start the calibration. This will ensure accurate measurements. This consists of checking the alignment of the measuring system, calibrating the force and torque sensors and the determination of the zero-gap position, finishing with a motor adjustment.

- adjust upper drive inertia in order to compensate acceleration torque
- adjust upper measuring system inertia in order to compensate acceleration torque.
- adjust upper motor in order to compensate residual friction (motor and encoder adjustment)

The device consists of a measuring system, that comes in different forms, such as the concentric cylinder, the cone-plate or the parallel plate. The measuring system needs to be handled carefully as the software of the device assumes that the measuring system is perfectly symmetric. Because the experiment requires to work with light, the measuring system must be made of a transparent material. A new measuring tool was manufactured

using a flat round disk made of borosilicate glass. The glass disk is connected to a rotating shaft and forms a new parallel plate spindle. Because this is an unknown measuring system for the software, it needs to be implemented into the software. After implementation and calibration, the test method can be established. Different material properties can be measured during the test, including viscosity, shear rate and shear stress, which are the main parameters in this experiment. Temperature can be controlled, but evaporation of the fluid can occur and must be checked throughout the experiment. The test method can be adapted to the required procedure, such as varying or constant shear rate, the sample rate of the data acquisition and many other options. Once the test method is entered in the software, the tests can start. The sample can be loaded onto the zero-gap positioned stationary surface. The sample consists of algae suspensions discussed previously in chapter 3. The device will register its measurements in tables. The specific procedure is discussed in more detail in section 5.1.3.

The rheometer requires careful handling by the user, but the user must as well be careful with the interpretation of the data. The instrument has a minimum torque T_{min} limitation that it can measure [34]. The torque range being from $0.5\,nNm$ to $230\,nNm$, within this range the rheometer remains stable. This is especially of importance with biological systems. At a torque above this minimum limit condition, the data measured is acceptable [34]. The torque T of the rheometer is related to the dynamic viscosity η through $\eta = \frac{2hT}{\pi R^4 \Omega}$, with the shear gap h, radius R and angular velocity Ω. The minimum measurable viscosity depends on the torque required to move the sample. Surface tension is also responsible for limitations in the torque measurements, resulting in a decreasing minimum measurable viscosity with increasing shear rate [34]. The gap size of the rheometer can influence the acceptability of the measured data and should be at least ten times the diameter of the particles immersed in the sample [34]. The device assumes a homogeneous shear flow, without the presence of air bubbles. The sample has to be uniformly distributed under the measuring system.

Additional accessories for a rheometer can enhance its capabilities and allow for more precise or specific measurements. Some common accessories include different types of measuring geometries, such as concentric cylinder, cone plate or parallel plate setups, which can accommodate various sample sizes and viscosities. Temperature control units are also common accessories, enabling measurements at different temperatures to study the effect of temperature on material properties. A heat insulating head is an accessory that maintains the temperature of a sample during measurements. In this thesis, an additional accessory is added, namely a light source for the purpose of phototaxis of the algal sample. The choices for the accessories are discussed below. There are important requirements to keep in mind when designing an experimental setup for the inclusion of external light in rheology.

- 45° requirement: align algae parallel and orthogonal with respect to the shear flow.
- Phototaxis: light source and light guiding system
- Geometry of rheometer: circular and size limitations
- Light pollution: dark surroundings
- Measuring system of rheometer transparent for optical access

5.1.1 Transparent Parallel Plate Measuring System

For the experiments, a parallel plate configuration is chosen. Because light needs to illuminate the sample, the measuring device must be transparent to get optical access to the algae. Therefore, it is made of borosilicate glass. The liquid sample consists of small, self-propelling particles, making a cone-plate more suitable, because a constant shear rate would be achieved throughout the sample. It is also known to work better for fluids with

rigid particles, because it prevents the particles from collecting at the edges. However, this measuring system is not used for simplicity of the design. The plate is made of glass, making it more complex and expensive to create in a cone geometry. Besides transparency, the plate must be perfectly round, transparent and free of blemishes, to assure the results obtained by the rheometer are valid. A glass plate containing imperfections can lead to incorrect measurements by the device and consequently provide wrong results. The parallel plate measuring system is made by gluing the glass disks on metal tips that are to be fixed on the rotating spindle of the rheometer. The different sizes made are $50\,, 60$ and $70\,mm$. Figure 5.1 illustrates both the original parallel plate made from stainless steel and the new glass tool custom-designed for this study.

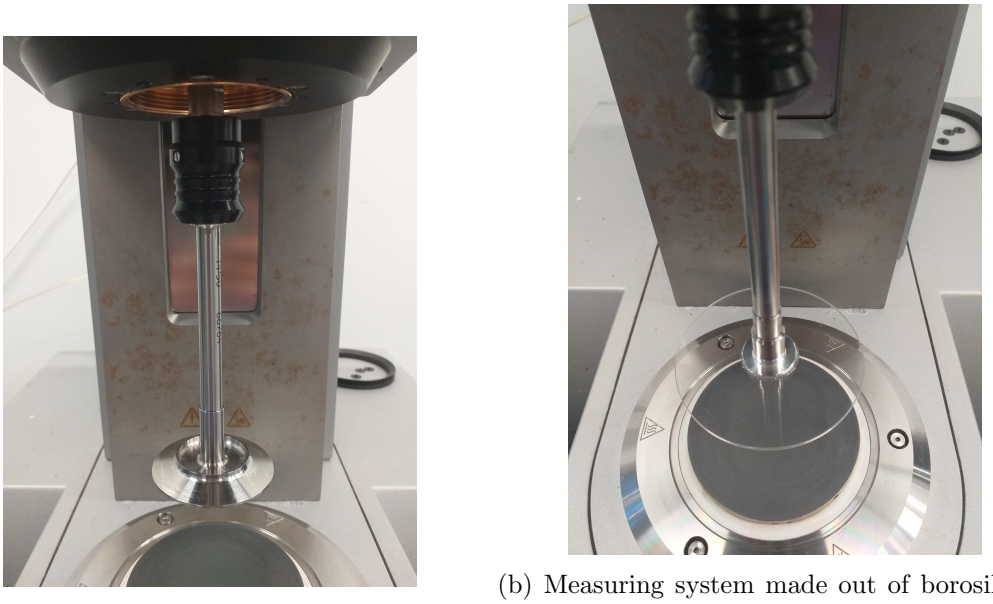

(a) Measuring system made of stainless steel.

(b) Measuring system made out of borosilicate glass.

Figure 5.1: The measuring system is the accessory attached to the rheometer that exerts a torque on the fluid sample. The standard stainless steel tool has a $50\,mm$ diameter.

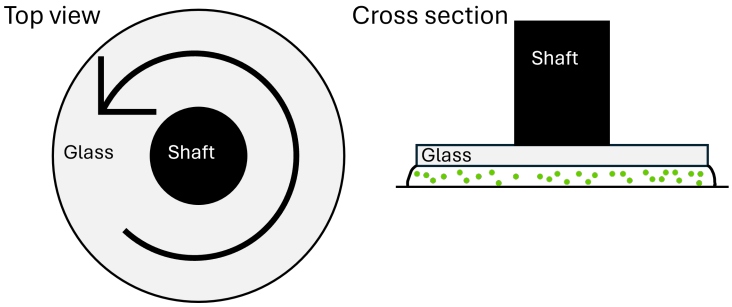

Figure 5.2: Top view and cross section of the measuring system of the rheometer. Representation of turning element.

5.1.2 Experimental Setup: Light-Control System on Rheometer

The purpose of the optical accessory is controlling the directional motion of the algae within the sample by creating a phototactic response. In order to obtain the right orientation of the organisms, the light rays need to penetrate the sample in the correct angle. One way to guide light towards the right incident angle is by creating tubes through which light rays can travel, such as in the previous experiment of the 3D imaging. Adding light guides around the shaft of the rheometer, adds some difficulties in the design. Firstly, in

order to illuminate the entire sample on the rheometer, the light guiding tubes need to encircle the shaft, forming something similar to a funnel seen from the side or by looking at the cross section, see figure 5.3. The next step is to look at the orientation of the algae required for this study. The algae needs to be aligned with or orthogonal to the extensional axis of the shear flow that is applied by the rheometer, which is at a 45° angle, which comes from the straining motion in the shear flow. This means that light rays must have this incident angle inside the algal sample. The light source encounters the glass from the measuring system of the rheometer. Consequently, the light guiding tubes are tilted the same way as in the experimental setup in chapter 4. Additionally, the funnel must be internally divided with walls to create a rectangular tubes-like shape. These must follow the direction of the applied rotational shear flow, meaning that the tubes are tangent on the top of the rotating surface of the measuring system. Summing up the rheometer's shear flow applied in an encircling motion and the angle of refraction, a structure of tubes serve as light guides and are created in a circular pattern, with each tube illuminating a part of the surface above the sample, see figure 5.4.

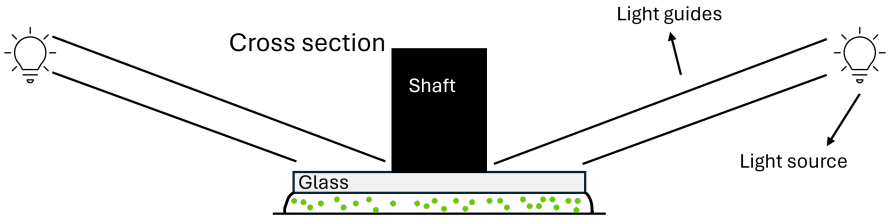

Figure 5.3: Cross section of funnel-like light guides.

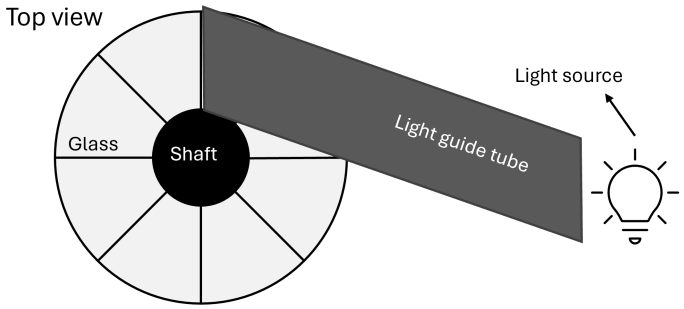

Figure 5.4: Top view of tube-like light guide illuminating a part of the surface of the measuring system.

5.1.2.1 Light Guides

The experimental setup is built in different stages on top of the rheometer. It is valuable to recall the experimental requirements mentioned at the beginning of this section. Phototaxis is obtained by light traveling through light guiding tubes that make sure to guide the light into the direction that causes the algae to align with and orthogonal to the extensional axis of the shear flow, which fulfills the 45° requirement. The rheometer causes dimensional limitations to the setup and thus complicating its design. The rheometer rotates and is circular. Therefore, the light guides are designed in a way to surround the rotational system of the rheometer, while letting the spindle rotate freely. A circular pattern of light guiding tubes is created with an inner diameter of 25 mm in which the spindle rotates. The rheometer has a circular design but is also limited in height. When it is powered on, the measuring system is fixed to a stand that needs to move vertically. During sample preparation, the stand descends to a shear gap of 1 mm, which restricts the available height for the setup. Additionally, there is a surface boundary at the back

of the rheometer that further limits usable space. As a result, the tubes can only have a total length of $8\,cm$.

Another limitation arises specifically to take into account the operations required for the sample preparation. First, the algal sample is placed on the stationary surface, see figure 5.9a followed by lowering the measuring system to the required shear gap, see figure 5.9b. In the process of vertical motion, it is essential that the device remains unobstructed by any objects. This requirement is critical, as the light guiding system is intended to be positioned directly above the glass component of the measuring tool. Therefore, a specific sequence of actions must be adhered to during experimental procedures: first, the sample should be placed; next, the measuring system must be lowered to the shear gap; and finally, the light guiding system can be positioned above the glass. To facilitate this process, the design of the setup should allow for the efficient placement of the light guides around the spindle of the measuring tool, as well as their removal prior to lifting the measuring system for cleaning purposes. For ease of tube insertion, the circular pattern is divided into two halves, which can be assembled around the shaft of the measuring system and secured in a support, thereby creating a unified structure. This enhances placement and removal of the tubes above the glass surface of the measuring system, although care must be taken to not touch the spindle during insertion.

At each location within the sample on the rheometer, the algae must receive light from above at a 45° angle. A structure of combined tubes is designed in a circular pattern to guide the light in the right angle. Appendix C illustrates the tubes designed in SolidWorks. Each tube has the function to illuminate the section of the algal sample underneath. The slope of the tube is taken with respect to the midline of the surface section. Consequently, the algae see the light within an interval of angles. The more tubes present in the design, the smaller the interval and thus the closer to meeting the 45° requirement.

5.1.2.2 Light Source

The light intensity and colour specify the choice of the light source. As elaborated in section 1.2.1, the green algae *Chlamydomonas reinhardtii* is sensitive to a spectrum of wavelengths corresponding to blue and green light. In experimental studies, white light was used and showed effectiveness in triggering a phototactic response [16][25][29][44]. According to study [44], the favoured light intensity of the green alga is at least $10\,\mu mol/m^2s$. Initially a white LED strip was chosen at an intensity of $I = 14.29\,\mu mol/m^2s$. The LED strip is connected to an Arduino, controlling an on-and-off cycle. The Arduino is placed between the light source and a power supply. The intensity of the light source is dependent on the current passing through the light and can be controlled by the power supply. The $24\,V$ LED strip can handle a current of $1.4 - 1.5\,A$, but the variation of the intensity is limited to this maximum intensity, which was only $5\,\mu mol/m^2s$ at the exit of the light guide. Another light source was chosen later in the process. This concerns a blue LED Phlatlight PT-121-B-L11-EPG from Luminus, which is a small, flat light with a great ability to achieve high intensities, that cannot be attained by common LED light bulbs. With their easy manipulation, 12 of these flat lights are connected to each other in series and joined to the same Arduino. Altogether, the light must not exceed a current of $2.5\,A$ for safety reasons. Sufficient power is required to provide the lights with a voltage of $36V$, which is provided by the power supply in figure 5.5. The intensity measured through the tube and the glass of the spindle is $75\,\mu mol/mm^2s$. These lights heat up with increasing current, necessitating sufficient cooling. An aluminium plate of a $2\,mm$ thickness is laser cut and attached to each light with the purpose to conduct heat away.

5.1.2.3 Manipulation of the Light-Control System

A frame is designed to support the tubes, as well as the light source and can be viewed on figure 5.6a. The base of the frame is a ring, which rests on the rheometer and does

Figure 5.5: Power supply providing sufficient power to 12 blue LED lights

not need to be removed at every sample preparation. It consists of two squared bars and two metal threads. The function of the threads is to adjust the height of the support in which the tubes lay, according to the thickness of the sample and the thickness of the glass parallel plate. The support holding the tubes and the light source is a ring as well and can slide up- and downwards over the squared bars of the frame, while turning the threads. The LED strip is adhesive and can stick on the inside of the up- or downwards moving support at the entrance of the tubes. The three parts of the structure are 3D printed, as it has a complex shape and requires to be lightweight to be carried from the lab to the rheometer. The plastic material can melt due to the heat radiated by the LED Phlatlight. In order to prevent this from happening, some spacing is placed between the light source and the tube, using a metal nut and ring, see figure 5.7, which prevent the LED source from touching the plastic.

(a) Experimental setup with blue LED Phlatlight.

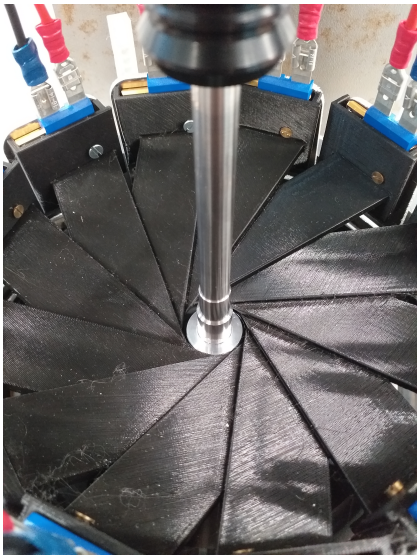

(b) Top view of experimental setup with blue LED Phlatlight with focus on surrounding the spindle.

Figure 5.6: Experimental setup with blue LED Phlatlight on top of the rheometer.

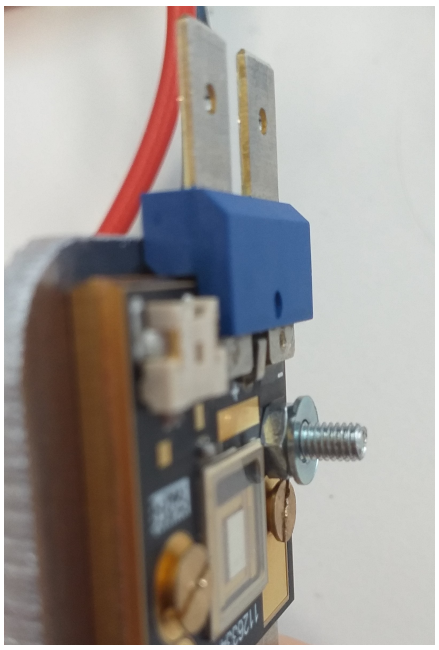

Figure 5.7: Spacing required between Phlatlight and tube to avoid melting of the 3D printed plastic acquired by metal nut and ring.

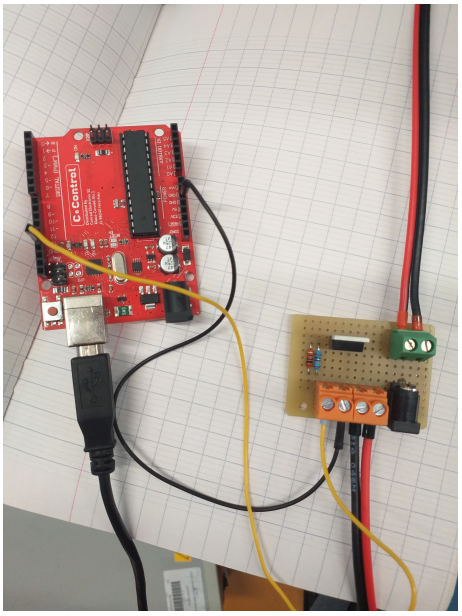

Figure 5.8: Arduino connection used to attach LED strip and LED Phlatlight.

5.1.3 Experimental Procedure for Light-Controlled Rheology Experiment

The rheometer measures the viscosity of the algal sample between the parallel plates. The multiple elements required for this experiment are the algal sample, the light-control system and the rheometer. The light-control system is placed on top of the rheometer and is thoroughly described in section 5.1.2. Here, the experimental procedure is detailed for the rheology experiments. Overall, the steps that must be taken when doing experiments are as followed. After the calibration, the first step is the sample preparation. This consists of deposing the algal sample on the stationary plate of the rheometer and enclosing the algal sample between the two parallel plates, mentioned in 5.1.3.1. The next step is to place the light guides with the light source on top of the glass measuring system. This is followed by the rheometer measurement that generates a signal for the viscosity, discussed in 5.1.3.2.

5.1.3.1 Sample Preparation

During the experiments, the external light will be blocked as much as possible, in order to eliminate light pollution from the surroundings to ensure that the algae do not respond to any unwanted light. A fabric is used to block the surrounding light, because the rheometer is in a bigger room used by multiple people. Although the light in the room was off, external light could enter through a window. The fabric covers the setup into the dark. For this experiment, the algal sample is grown in TAP in order to achieve higher concentrations. Throughout the experiments, a range of volume fractions will be used from 0.5% until 2% and thus remaining in the diluted regime. Too high cell concentrations may lead to light scattering and absorption, reducing the intensity of the light and blocking light for the organisms positioned at the bottom layers of the sample. The temperature is kept constant during experiments and is set at $T = 28°C$. Warm temperatures enhance the activity of the algae, which will be beneficial when looking for a response.

Preparing the sample on the rheometer is an important step. The first step is to transfer the right quantity to the stationary surface, than lowering the measuring system

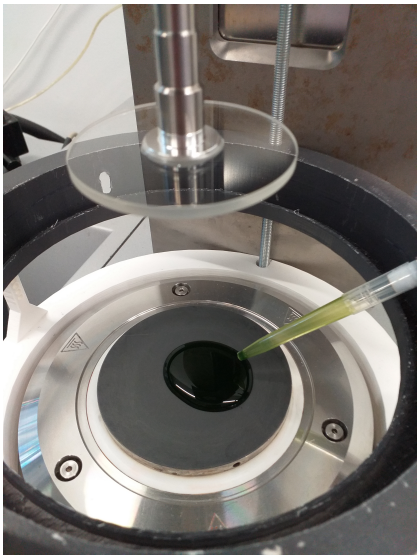

(a) Injecting the sample on the stationary plate of the rheometer using a pipette.

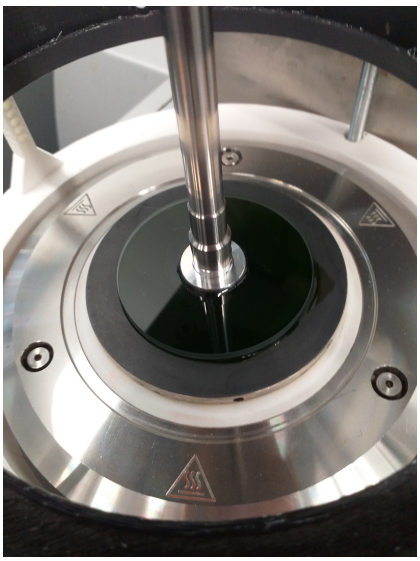

(b) Sample sitting between the stationary plate and the measuring system ready to be measured at a $1\,mm$ gap.

Figure 5.9: Sample preparation before starting experiments requires careful attention to quantity and impurities.

into confining the algal sample between the to parallel plates as illustrated in figure 5.9. The shear gap of the rheometer is the spacing between the two parallel plates in which a fluid sample is sitting. This spacing between the stationary plate and the measuring system is fixed at $1\,mm$ for all experiments. The sample must not contain bubbles or unwanted particles such as dirt or flocculation. Having a transparent tool provides to see immediately if there are any bubbles formed in the sample. Bubbles may appear when the sample evaporates, which happens at higher temperatures. To prevent this from happening during experiments, the measuring system is first lowered, before heating the sample at $28°C$. This temperature activates the organisms, enhancing their activity and movement.

5.1.3.2 Signal Generation and Analysis

By inserting a flow procedure in the software of the rheometer, the flow velocity can be set. The shear rate was initially set at $10\,s^{-1}$. After reconsideration, lowering the shear rate could be beneficial in obtaining a phototactic response from the algae. A relatively high shear rate could prevent the algae from reorienting, as the flow is too strong and pushes the organisms to rotate with the shear flow between the parallel plates. Therefore, the method was expanded into measuring low shear rates of $1, 4$ and $10\,s^{-1}$. In order to align the organisms orthogonal to the extensional axis of the shear flow, the measurement system can rotate in the opposite direction, which is set in the software by the shear rates $-1, -4$ and $-10\,s^{-1}$. The experiments performed are time dependent at a constant shear rate. The light source is switched on-and-off using the Arduino, in periods of 15 seconds light off, as this is the time needed for the algae to forget their phototactic response. Approximately three seconds are needed for the algae to reorient themselves towards the light source. The light is therefore switched on for 6 seconds. The rheometer measures the viscosity, which is done at a sample rate of $10\,Hz$ during 4 minutes to ensure that the measuring tool could finish complete rotations. An observation that was made in the previous experiment in section 4.2, was that the cells tend to swim upwards towards the light and collect at the top surface. This means that precautions must be taken for the experiment under the rheometer, where a similar phenomenon could occur. If cells collect

at the top surface, the viscosity measured by the rheometer would not be reliable, as the sample will not be homogeneous in this particular case.

Afterwards, some manipulation is involved in the data analysis. A time ranging signal is inspected visually to search for viscosity increments in the positive shear measurements and viscosity decreases in the negative shear measurements. This corresponds to the applied stresslet caused by the alignments of the algal orientation. Before measuring any algal samples, the transparent glass-made measuring system must be validated and quantified. This way, a correct data interpretation can be established for the generated data. The transparent tool is first characterised in section 5.2.

5.2 Validation of the Transparent Parallel Plate Measuring System of the Rheometer

The importance of having a transparent measuring system is to allow light to penetrate the fluid sample, such that the sample can be illuminated. The light-controlled rheology consists of multiple elements. Discussed at the beginning of this chapter, a setup was designed to guide the light in a specific orientation onto the algal sample, complemented by the rheometer and its new, glass-made measuring system. The use of the light-control design is validated by the previous experiment with the 3D imaging in chapter 4, where a tube was used with the same geometrical properties. This resulted into a 45° angle of the algae's swimming orientation. Secondly, the measuring system of the glass-made measuring system must be validated and characterised. This validation consists of finding out whether the glass-made spindle can be used for accurate rheology measurements.

5.2.1 Viscosity Validation of Newtonian Samples

The validation assessment consists of finding out if the new measuring system, now constructed of borosilicate glass instead of stainless steel, can meet the measuring performance of the metal measuring system and provide for correct results. Figure 5.1 shows both metal and glass spindles. Essentially, the viscosity measured by the new system should match the viscosity measured by the metal system. To conduct this evaluation, the spindles are attached to the rheometer to measure the viscosity. The validation is performed on Newtonian fluid. The two fluids tested under rheology are distilled water and a ficoll solution, with a low and high viscosity respectively. A ficoll solution is obtained by gently mixing the powder ficoll PM 400 with water. This evaluation enables to compare the measuring systems and will confirm the performance of the new measuring system in relation to the standard stainless steel tool. Three different measuring systems are tested for the borosilicate glass disks with diameters of 50, 60 and 70 mm and one stainless steel tool of 50 mm. The metal tool is available with the rheometer, but the glass tools were made by gluing a metal tip exactly in the middle of the glass disk. The shear rate is linearly increased by the rheometer from 1 s^{-1} to 100 s^{-1}. The increasing shear rate during the experiment is to verify that the measuring system is indeed measuring a Newtonian fluid as should be the case for both substances. By verifying the shear stress, a linear relationship should exist between shear rate and shear stress. Another property is the constant viscosity throughout the experiment. Besides matching the viscosity of the original metal tool, the viscosity measured by the glass tool should coincide with the viscosity found in the theory for the substances tested, with the dynamic viscosity of water equal to $\eta = 0.89\,mPa \cdot s$ [43] at $25°C$ and of the ficoll solution $\eta = 20mPa \cdot s$ [3] at $20°C$. The rheometer calculates the average data acquisition for each individual shear rate by taking the average over one complete rotation of the spindle.

The first fluid being tested is the low viscosity distilled water. The data that is obtained by the rheometer is collected into a graphic presented in figure 5.10. Besides distilled water, also the culture medium of the green algae was tested, namely TAP, shown in figure

5.11. The viscosity of both fluids remains constant with an increasing shear rate. Correspondingly, the shear stress increases linearly. For water, the viscosity is $\eta = 0.89\,mPa \cdot s$ at a temperature of $25°C$. The viscosities measured by the original stainless steel tool measures a viscosity of $1.2\,mPa \cdot s$, followed by slightly decreasing viscosities using the glass made spindles. Noteworthy, is that the bigger the diameter of the measuring system, the closer to the actual theoretical value. Bigger diameters provide to measure low viscosities better than small diameters.

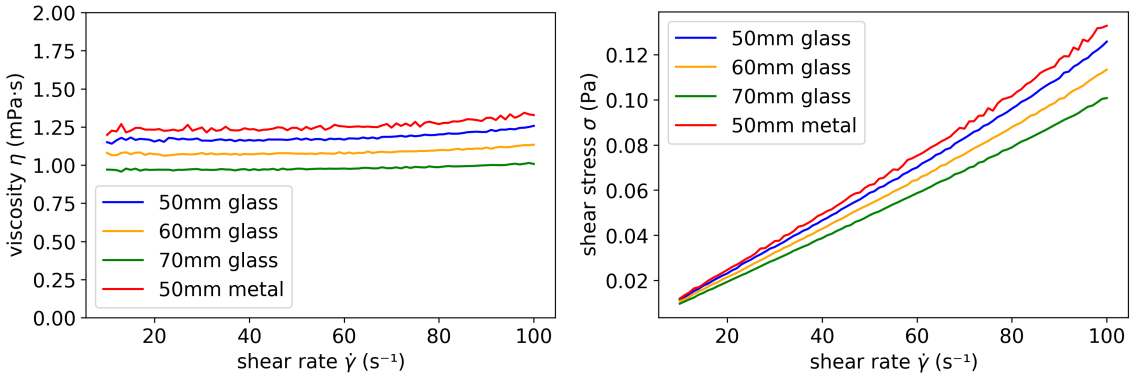

(a) Dynamic viscosity (b) Shear stress

Figure 5.10: Distilled water data obtained by the rheometer with 50mm, 60mm and 70mm diameter measuring system of glass, compared to the original measuring system of metal. The temperature is fixed at $T = 25°C$.

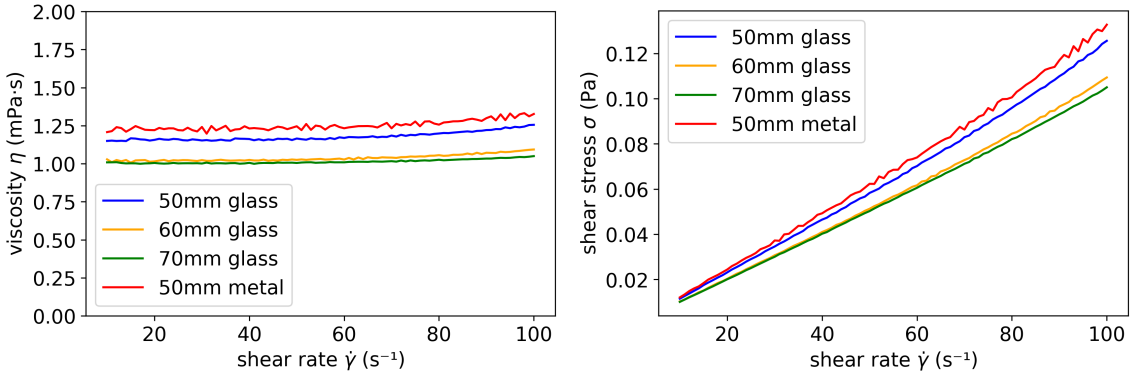

(a) Dynamic viscosity (b) Shear stress

Figure 5.11: TAP data obtained by the rheometer with 50mm, 60mm and 70mm diameter measuring system of glass, compared to the original measuring system of metal. The temperature is fixed at $T = 25°C$.

The next fluid being tested is the high viscosity fluid, a ficoll PM 400 solution at $20\%\,w/v$. The mixture is tested under the rheometer using the different tools. The results for the viscosity are published in figure 5.12a. The viscosity of the solution should be $20\,mPa \cdot s$ [3] at a temperature of $20°C$.

Analysing the evolution of the shear stress during the measurement can tell more about a fluid's behaviour. Shear stress arises when a fluid is in motion due to a force applied on it which is deforming the fluid. Newtonian fluids have a linearly increasing shear stress with increasing shear rate. This was expected for the tested fluids. As can be seen in the graphs of figures 5.10b, 5.11b and 5.12b, the shear stress did increase linearly with increasing shear rate. This validation experiment verified if the newly glass made measuring system could meaningfully measure fluids and that the data was reasonable. Consequently, the tool could be used with more confidence on the applications of the fluid

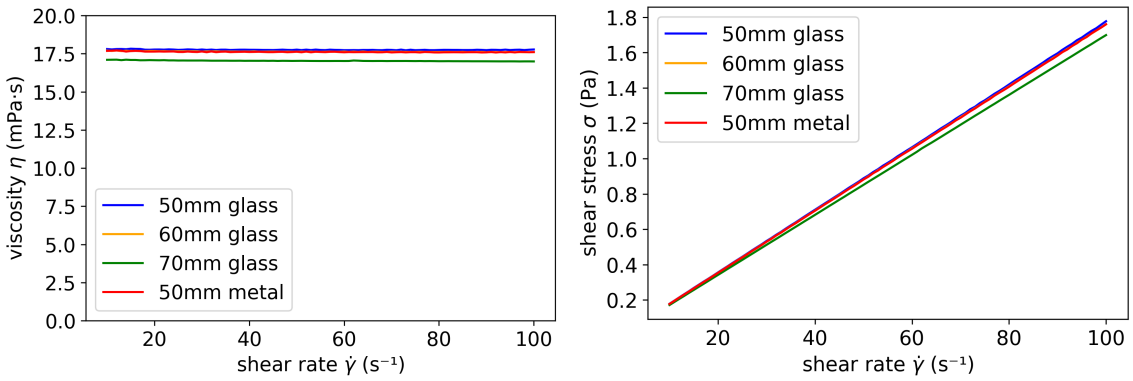

(a) Dynamic viscosity

(b) Shear stress

Figure 5.12: Ficoll PM 400 solution data obtained by the rheometer with 50mm, 60mm and 70mm diameter measuring system of glass, compared to the original measuring system of metal. The temperature is fixed at $T = 20°C$.

containing algae suspensions.

5.2.2 Signal Characterisation of Constant Shear Measurements

The light-controlled rheology experiment will include the generation of a time-evolving signal, which is achieved at a constant shear rate. Therefore, the signal obtained by the glass tool is characterised using distilled water. This step is to develop the procedure for the signal generation with the rheometer. The experiments require a time dependant measurement at a constant shear rate. This allows us to determine whether the phototactic response to the light results in a change in viscosity. A sample rate of $10\,Hz$ is chosen to capture more detail within the signal of the rheometer. The shear rates are fixed at $1, 4$ and $10\,s^{-1}$, which will be used for the rheology experiment on the algae.

A difference between the constant measurement and increasing shear measurement is the sample rate. The constant shear measurements have a clear periodicity, see figures 5.14a, 5.15a and 5.16a, which did not appear when data was acquired over a full spindle revolution. Additionally, more noise is present when the sampling rate is increased. The calibration method was therefore revisited in an attempt to improve the signal. The third step in the calibration process is the motor adjustment. Two methods exist: the standard motor adjustment and an advanced motor adjustment. The results of the measurements obtained using both calibration methods were compared and are represented in figure 5.13. The periodicity remains present in the generated signal, but is slightly improved as it has a smaller amplitude and is more smooth. It is therefore employed to each calibration performed for this research.

More focus is brought to the periodicity observed in the data. A long-duration experiment with the glass tool is conducted for one hour on water. Through this extended measurement, the aim is to determine whether the periodic behaviour reduces over time or persists through multiple revolutions and try to correlate the frequency to its source. This experiment is done for all three shear rates $1, 4$ and $10\,s^{-1}$. Figures 5.14, 5.15 and 5.16 represent the long-run measurement on water at shear rates of $1, 4$ and $10\,s^{-1}$ respectively. The blue curve represents the original viscosity measured, while the orange curve represents the Savotzky-Golay filtered data of the viscosity. In order to determine what frequencies are present in the signal, the power spectrum of the signal is calculated. While high frequencies correspond to noise that originates from the measurement itself, the lower frequencies are related to periods associated with the tool's geometry. As the glass disk is glued to the metal tips, there is a possibility that the spindle is not perfectly balanced. This means that one complete revolution is associated with a periodicity in the signal and this is viewed in the power spectrum. The frequency associated to the tool's

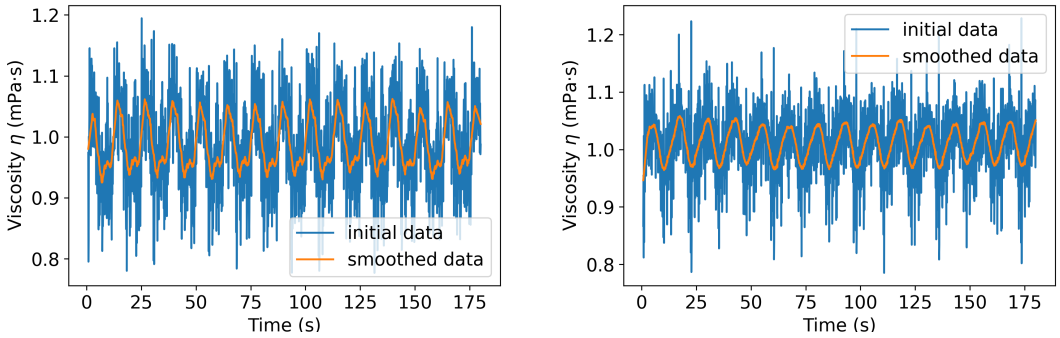

(a) Standard motor adjustment

(b) Advanced motor and encoder adjustment

Figure 5.13: Comparison of adopting the advanced motor adjustment during the calibration. The dynamic viscosity of water is measured at a shear rate of $10\,s^{-1}$.

revolution can be calculated through $f_{tool} = \frac{RPM}{60}$, with $RPM = \frac{\dot{\gamma} h}{2\pi \frac{2}{3} r}$. The shear rate is imposed at 2/3 of the radius of the measuring system of the rheometer, which is at a shear gap $h = 1\,mm$. A regular period corresponds to a complete rotation of the measuring system. While the power spectrum provides insight into the recurrent frequencies in the measurement, it is also valuable for the light-controlled experiment with the algae. It will ensure that the period of the light cycle of 21 seconds does not coincide with a frequency naturally present in the system.

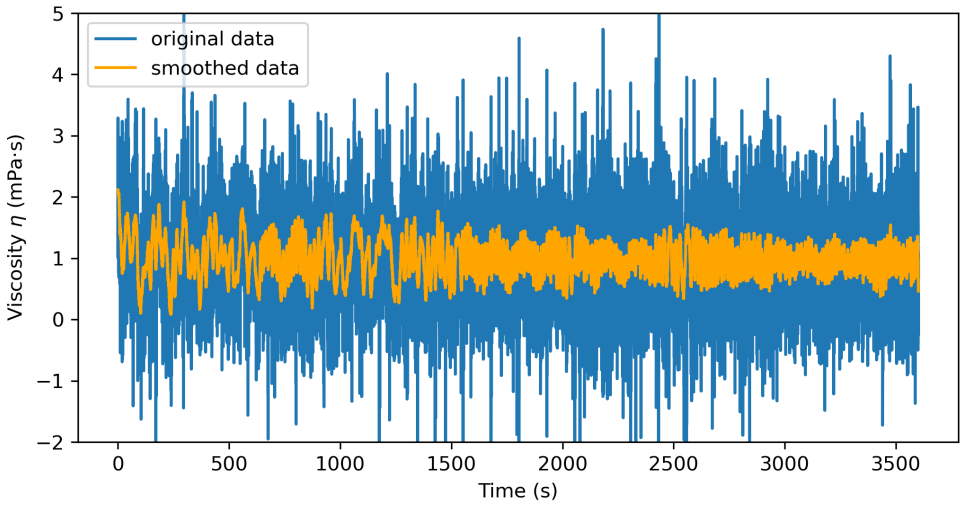

(a) Time-domain

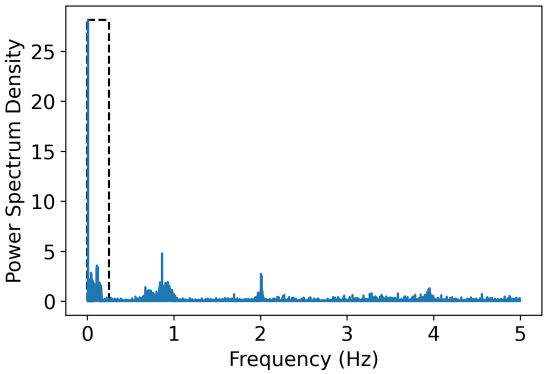

(b) Power density spectrum

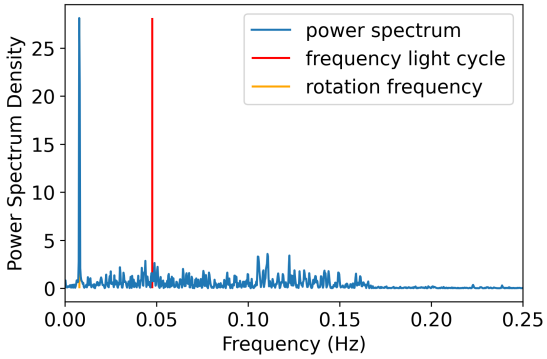

(c) Power density spectrum focused on low frequencies

Figure 5.14: Long-run measurement on water at $20°C$ for one hour at a shear rate of $1\ s^{-1}$.

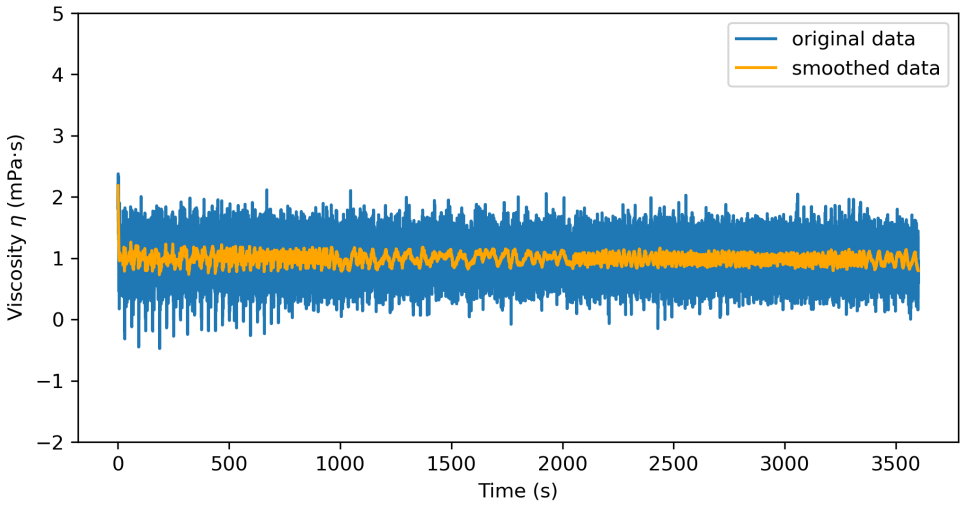

(a) Time-domain

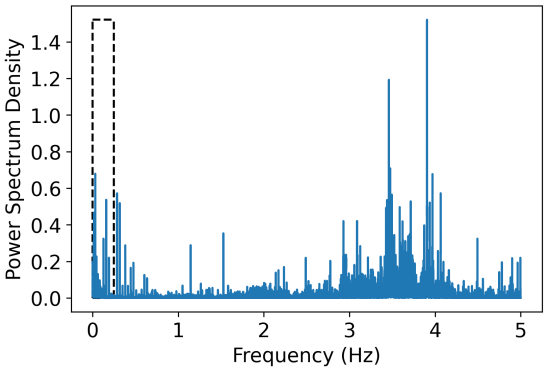

(b) Power density spectrum

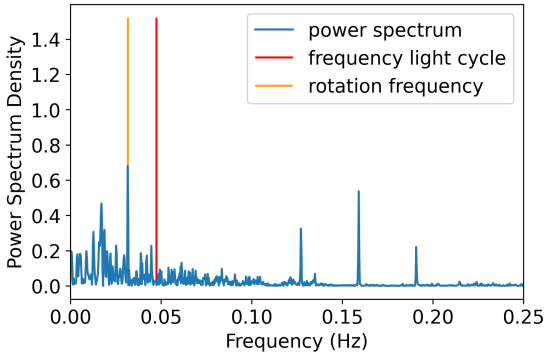

(c) Power density spectrum focused on low frequencies

Figure 5.15: Long-run measurement on water at $20°C$ for one hour at a shear rate of $4\,s^{-1}$.

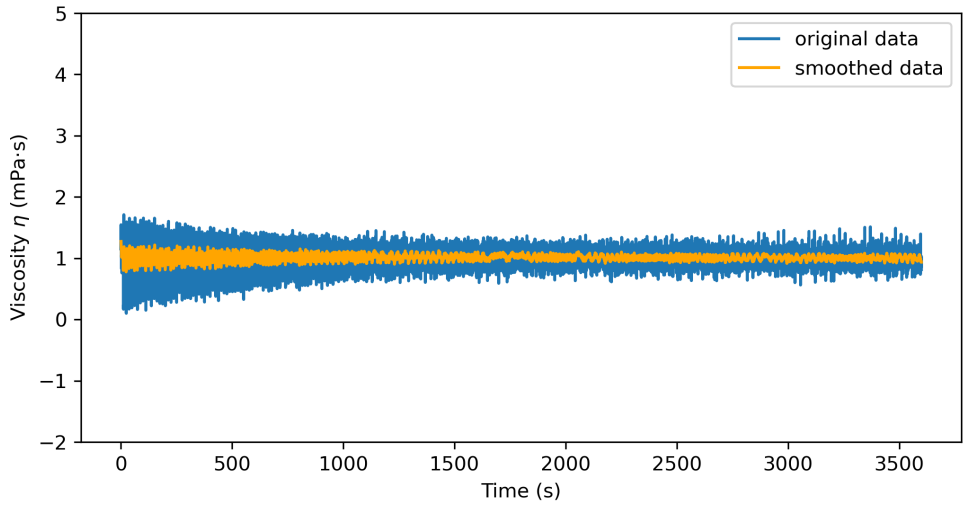

(a) Time-domain

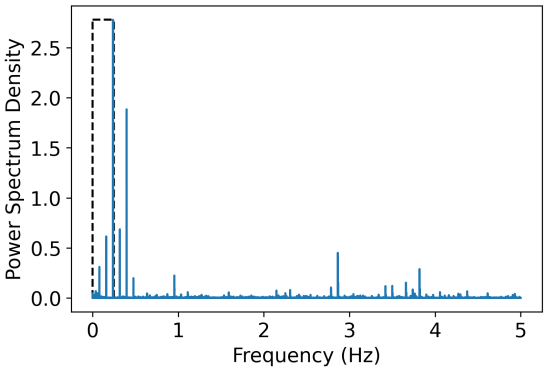

(b) Power density spectrum

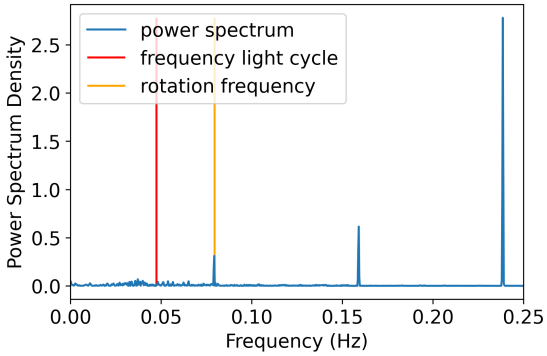

(c) Power density spectrum focused on low frequencies

Figure 5.16: Long-run measurement on water at $20°C$ for one hour at a shear rate of $10\,s^{-1}$.

A general observation made in all constant shear measurements was the presence of unstable data acquisition at the very start of the measurement. At the start of the measurement, until 0.8 second, the acquired viscosity fluctuated significantly, before settling to a reasonable amount. This phenomenon is called the transient regime [24]. As the fluid is stationary at the start, it needs a transition period to attain a shear flow. The transient regime was removed for all the measurements, including the algal samples. Figure 5.17 shows how the transient regime interferes with the Fourier analysis.

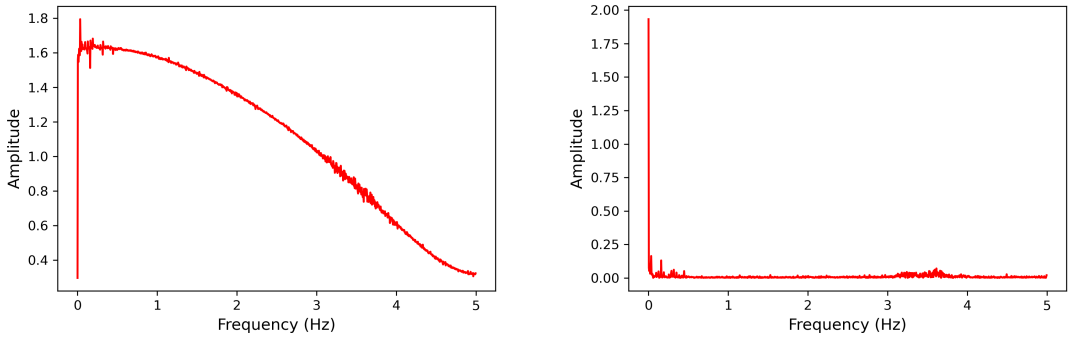

(a) Preserve transient regime

(b) Eliminate transient regime

Figure 5.17: The graphics show the effect on the Fourier transform of a signal when the transient regime is maintained and removed. The viscosity at the start of the measurements fluctuates significantly and results in unexplainable behaviour in the Fourier Transform as seen in 5.17a.

5.3 Results of the Experimental Study on the Viscosity of the Light-Controlled Algal Sample during Rheology

The final experiment was the light-controlled rheology performed on the algae. The experiment involved combining all the different elements discussed: the light-control system, the algal sample, and the rheometer with its glass-made measuring system, which was needed to illuminate the biological suspensions in the sample underneath.

Two light sources were tested: the white LED strip and the blue LED Phlatlight. As the white LED strip did not meet the required light intensity, the light source was upgraded to a blue LED Phlatlight, which could achieve much higher intensities. The microscopy experiment with the light-controlled algae was performed using a green and white LED Phlatlight, as described in chapter 4. During the 3D imaging experiments, the blue light source was unavailable in the lab, the algal orientation with the blue LED light source could not directly be measured. With wavelengths close to those of green light, blue light is known to be an efficient light source for the phototaxis of *Chlamydomonas reinhardtii*.

The time ranging signals present the original data obtained for the viscosity and are found in figure 5.18 and in the figures in appendix D and E. The algal samples were tested both in a dark environment and under light-controlled conditions. The light-controlled experiments are indicated with red vertical lines marking the time when the light was switched on. It serves as a physical indication of when a phototactic response could be expected to happen. The noise naturally present in the signal makes the direct observation of the viscosity unlikely. The noise is unpredictable and varies from measurement to measurement. The signals were smoothed, but as this removes outlying points, it could possibly remove an impulse resulting from phototaxis. Consequently, advantage is taken of the physical information regarding the on-and-off cycle of the light, which lasts 21 seconds. This means that a periodic impulse could be expected every 21 seconds. The time-domain is converted into a frequency-domain. More specifically, the power spectrum is analysed for these experiments. The amplitudes in the power spectrum represent the distribution of power at different frequencies. Both power spectra and time-domain signals are presented in appendix D and figure 5.18. The smoothed, orange data in the time-domain signal is a tool for visualising certain periods that appear in the power spectrum. The orthogonal alignment is achieved by reversing the shear rates and are shown in appendix E. The frequencies of the power spectra go up to the Nyquist frequency at 5 Hz, which corresponds to half the sample rate. An analysis is done on the noise of the viscosity measurement

in order to quantify its impact and magnitude in the power spectrum. The standard deviation of the noise of the time ranging viscosity signal is calculated for the positive shear measurements [32]. Then, new random data is generated in Python with the same standard deviation and sampling rate. Following from this newly generated random data, the power spectrum is computed. At this point, this power spectrum contains only random data similar to the noise of our viscosity measurement. The magnitudes in the power spectrum are thus random as well and estimate the magnitude of the power peaks of the noise. New random data is created every time the code is ran. The different power spectra provided a quantification of the maximum expected power for noise. This way, the power of the noise could be better distinguished from the power peaks at the light cycle frequency. Because each viscosity signal is unique and noise interferes irregularly, the amplitudes vary throughout each experiment. Therefore, the amplitude of each signal was observed and separately translated into Python through random noise. It should be kept in mind that standard deviations and noise interpretation are approximations. The power amplitude of the noise is mentioned in the figure captions of the power spectra figures. When the peaks are larger than the power magnitude of the noise, it means that the rheometer has captured a signal that could possibly be related to the light signal. It is uncertain whether conclusions can be made on the light-cycle frequencies that have a peak increment lower than the estimated power magnitude of the noise. Additionally, signal-to-noise ratios are low in the experiments, meaning that the signal is not detectable in the noise of the time-domain [32]. Therefore, the best way of viewing the light response is through the power spectrum.

The data for a volume fraction of 0.5% at a constant shear rate of $4\,s^{-1}$ is shown in figure 5.18. This figure shows the time-ranging measurement of the algal sample in a dark environment and during light-control. The power spectra of both are presented next to the time-ranging signal. A viscosity increment was expected every 21 seconds due to the reorientation towards the light. As mentioned earlier, noise interrupted the detection of a possible viscosity increment. Therefore, the power spectra are used to see if a periodic signal appears at the frequency of the light-cycle, indicated in the power spectra with a red vertical line. The power magnitude of the dark and light-controlled experiments were compared at this frequency. An increment in the peak is present, which is larger than the estimated power magnitude of the noise, which is at 0.08.

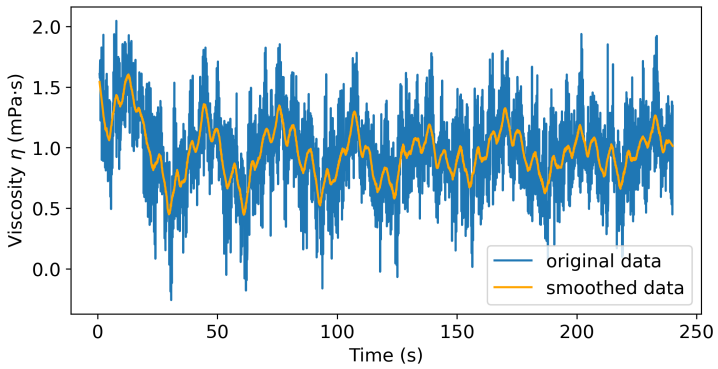

(a) Time-domain for dark suspensions

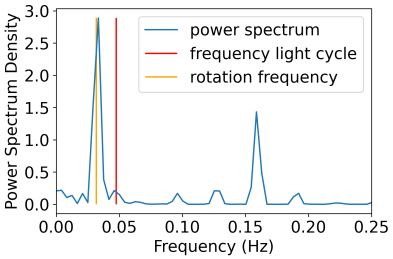

(b) Power spectrum dark

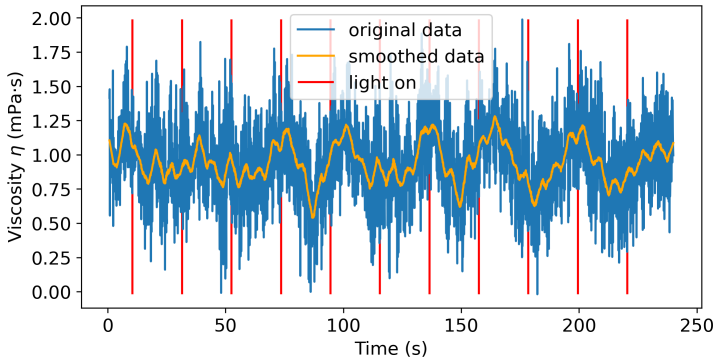

(c) Time-domain for light-controlled suspensions

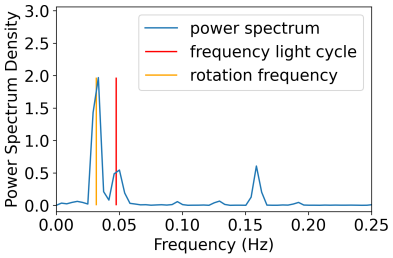

(d) Power spectrum light-control

Figure 5.18: 0.5% algal sample at a shear rate of $4\,s^{-1}$. Noise power amplitude for the dark algae is 0.08 and for the light-controlled algae is 0.08.

An additional quantification was performed on the strength of the viscosity. The peaks of the power amplitude correspond to the viscosity measured during the experiment. The amplitude at the light cycle frequency was converted to the corresponding viscosity $\eta_{experiment}$ added through the light response. The viscosity η_{model} was then modeled using the flagella beating frequency to calculate the velocity $u = f_{beating}l = 800\,\mu m/s$ from [47] with $l = 10\,\mu m$. All the values for the positive shear rate experiments were added in table 5.1. The two viscosities were compared, showing that some experiments did achieve a viscosity of the same order, which could be an extra indication that the peaks in the power spectrum are indeed related to the light-response.

Shear Rate	Cell Concentration	Amplitude	$\eta_{experiment}$	η_{model}
$\dot{\gamma} = 1$	0.5%	5	0.35	0.705
	1%	2	0.22	1.424
	2%	0.75	0.14	2.136
$\dot{\gamma} = 4$	0.5%	0.5	0.113	0.176
	1%	0.6	0.123	0.356
	2%	0.15	0.062	0.534
$\dot{\gamma} = 10$	0.5%	0.02	0.022	0.070
	1%	0.04	0.032	0.142
	2%	0	0	0.214

Table 5.1: Table displays the amplitude of the power spectrum at the peak of the light cycle frequency with the corresponding viscosity measured $\eta_{experiment}$ and the theoretical approximation for the viscosity $\eta_{model} = \frac{c\eta_{medium}ul^2_{flagella}}{\dot{\gamma}}$

5.4 Discussion of Light-Controlled Rheology Experiment

Up to now, this chapter has covered the experimental approach to the light-controlled rheology experiment and the results obtained by the rheometer. This experiment combines the light-control of biological suspensions of *Chlamydomonas reinhardtii* with a rheometer in order to measure the influence that the induced flagellar stresslet has on the viscosity.

The first topic addressed is the validity of the experiments. Multiple elements were validated separately and combined on the rheometer. The question is whether the combination of various elements resulted in the effect that was intended when applied to the rheometer. The procedure was performed in a consistent manner, including the culture, calibration and sample preparation, and it was ensured that the rheometer was manipulated correctly. The light-control of the algae was successful in the 3D imaging experiment of chapter 4. However, this was in a stationary flow, while in the current setup this had to occur in an externally applied flow. The flow may impact the organisms' ability to reorient themselves, introducing an unknown variable into the experimental setup. It remains uncertain whether the phototaxis can effectively counteract the flow [45]. To add validity to the procedure employed, theoretical factors were considered. An example is the shear rate that was lowered to balance the speed of the flow with the reorientation of the algae [45].

The next topic to discuss is the interpretation of the results and whether they match the expectations. The first results obtained were from the validation experiment of the glass-made measuring system described in section 5.2. The viscosity measurements on Newtonian fluids confirmed the reliability of the measuring system for measuring correct viscosities. Generating a constant shear measurement introduced noise into the system, complicating the analysis and necessitating a shift towards examining the power spectrum. A periodic frequency was distinguished in the signal, corresponding to the rotation of the spindle, indicating that it was not perfectly balanced. The measuring system was made by gluing the glass disks to metal tips and was therefore not perfectly symmetrical. Furthermore, the sources of other frequencies observed in the power spectra are not clear and made it difficult to characterise the measuring system. This adds ambiguity to the result interpretation from rheology with algae suspensions, because it becomes unclear if the signal viewed is a resultant of noise, or a frequency naturally present or if it is a result of the reorientation towards light. The initial expectation was a viscosity increase at a positive constant shear rate when light was turned on. It is unknown whether the signal will be a short impulse or if the viscosity change will persist, and how long the signal will persist. The only physical information is the time at which the light source is switched on and off. The time ranging viscosity signal was interrupted by noise, shifting the analysis to the power spectrum. Quantifying the noise as a power magnitude simplified the interpretation of the power peaks and provided a way to distinguish the noise from the signal. Removing the noise through smoothing using filters was not an option, as there was a risk that the phototactic response might be removed as filters remove outlying points. An increase in the power spectrum was observed in the light-control experiment, which was greater than the noise power amplitude. This could possibly indicate that the stresslet of the organisms did indeed contribute to variation in the signal. To determine if the magnitude of the increase is probable to be related to the reorientation of the algae, we quantified the added viscosity as shown in Table 5.1. The results indicate that the modeled viscosity are of a similar order of magnitude to the measured viscosity, suggesting that the increase could indeed be attributed to the reorientation of the cells. The negative shear experiments did not result in a power peak at the light cycle frequency. Additionally, multiple cell concentrations were tested, including a 6% volume fraction whose results are presented in appendix G, which show an increase in the power peak at the light cycle frequency, which could indicate the effect of added viscosity to the system.

It is difficult to interpret the signal clearly, because there was not an explicit viscosity increment observed directly. The specific signal being sought is unknown due to the lack

of experimental proof on the alignment of the algae. This means that the results could not be compared with other studies. Despite the lack of resources, a methodology was established by assembling the relevant theoretical concepts and experimental factors into the research methodology, including the shear rate, cell concentrations and phototactic characteristics of the green algae. A quantification on the power spectrum peak at the light cycle frequency proved that there is a possibility that a viscosity increment was indeed obtained. Future research involves studying the 3D motions of organisms under the shear conditions of the rheometer. This includes researching the shear rate that allows cell reorientation towards light within a shear flow. It would be beneficial to study this competition between the torque induced by phototaxis and the one within the shear flow. Designating the right range of shear rates that promotes the balance between the phototactic reorientation of organisms and the shear flow, and confirm their orientation under shearing conditions through 3D imaging will provide proper guidelines for future experiments in this field of research. Additionally, the characterisation of the measuring tool must be investigated to ensure clear signal generation. If the presence of the power peaks at the frequency of the light cycle do indeed correspond to the light response, this would support the current theory of the added viscosity.

Chapter 6

Conclusion

A fluid's properties are influenced by the presence of immersed particles, but the effect of self-propelling particles, such as organisms, enhance the stresses in the fluid system even more. The active stresslet that emerges from beating flagella is thought to be the reason behind the observed changes in properties of fluids including the viscosity. Through this research, the effect of the orientation of the green algae *Chlamydomonas reinhardtii* was analysed. The first part consisted of fixing the cell's swimming orientation by making use of phototaxis. Through a light guide system of tubes, the orientation of the organisms was aligned. This was then developed into a setup that can be placed on a rheometer that imposes a shear flow with a rotational motion. The viscosity was measured to find out if the orientation of the organisms influences the stress induced in the fluid system.

The theoretical framework in chapter 2 described the relevant concepts and introduced the hypothesis that is formed to point out the impact of the activity of organisms on the suspending fluid. Two research questions build up the concepts to be analysed in order to approach the hypothesis. The first question was if the swimming orientation of the green algae could be controlled. The 3D microscopy, elaborated in chapter 4, provided images with position and velocity vectors of the particles at each frame. An LED light source was used to control the orientation of the algae with phototaxis. This experiment was successful as different light sources resulted into an orientation aligned in a 45° slope. The second research question was if the viscosity of an active sample can be controlled. In the introduction in chapter 1, the concept of smart fluids was introduced, which is defined as a fluid whose properties can be manipulated intrinsically using external stimuli. The light-controlled rheology experiments in chapter 5 used light as the external stimuli to control the active fluid, but did not result in clear, explicit appearing viscosity increments. The occurrence of noise interrupted the interpretation of the results. A signal could have occurred, but would not have been detected by the amount of noise. By looking at the power spectrum, an increase in power was observed at the light cycle frequency of the multiple experiments. This is possibly caused by the phototactic response of the organisms. Viscosity was thus not controlled in a visible, detectable manner, but orienting the organisms did result in some effect viewable in the power spectrum.

The discussions suggested future work that involves the orientation in the light-controlled rheology and the characterisation of the measuring system. Further investigation would be required to specify if the occurrence of these peaks are indeed related to the orientation of the organisms towards the light. The rheometer could be inadequate to measure reliably the viscosity increment in a time-domain fluid system. Reducing noise in the rheometer is beneficial to the signal detection. Noise reduction could perhaps be achieved by connecting an instrument containing an AD converter to the rheometer software, but further investigation should be done regarding the contribution of this instrument [12].

Improvements that could be made in the experimental setup include the creation of light guides that resist high temperatures, in order to increase the light intensity of the blue LED lights even more. The use of a laser could strongly affect the orientation of the

organisms as the algae strongly remain in the laser spot. The laser generates an inhomogeneous concentration field that maximizes at the laser [8]. This effect is undesired during rheology, as the rheometer assumes homogeneous samples. Perhaps, another experimental method could be considered to analyse viscosity changes of orientational control of the algae using a laser.

This field of research is not widely investigated, resulting in the lack of scientific resources. Although the experiments accounted for correct conditions regarding the sensitivity of the rheometer, the lack of other experimental research provided a limitation in analytical knowledge. Furthermore, the absence of experimental research hinders our understanding of how organisms behave in a shear flow and the strength of their phototactic response. This research aimed to help contributing to construct experimental evidence in the hope to explore more of this microfluidic world.

Bibliography

[1] M.B. Akolpoglu et al. "Magnetically steerable bacterial microrobots moving in 3D biological matrices for stimuli-responsive cargo delivery". In: *Science Advances* (2022). DOI: https://doi.org/10.1126/sciadv.abo6163.

[2] Jorge Arrieta et al. "Phototaxis beyond turning: persistent accumulation and response acclimation of the microalga Chlamydomonas reinhardtii". In: *Scientific Reports* 7.1 (2017). DOI: https://doi.org/10.1038/s41598-017-03618-8.

[3] *Avantor is setting science in motion for a better world.* https://www.avantorsciences.com/ca/en/product/11231259/ficoll-pm400-cytiva.

[4] H.A. Barnes, J.F. Hutton, and K. Walters. *An Introduction to Rheology.* Rheology series. Elsevier, 1989. ISBN: 0-444-87140-3.

[5] G.K. Batchelor. "The stress system in a suspension of force-free particles". In: *Journal of Fluid Mechanics* 41.3 (1970). DOI: https://doi.org/10.1017/S0022112070000745.

[6] W. Borchard. "Properties of Thermoreversible Gels". In: *Berichte Der Bunsengesellschaft Für Physikalische Chemie* (1998). DOI: https://doi.org/10.1002/bbpc.19981021115.

[7] *DaVis – Software Solution for Intelligent Imaging.* https://www.lavision.de/en/products/davis-software/.

[8] J. Dervaux, M.C. Resta, and P. Brunet. "Light-controlled flows in active fluids". In: *Nature Phys* 13 (2017). DOI: https://doi.org/10.1038/nphys3926.

[9] S. Dupuis and S.S. Merchant. "Chlamydomonas reinhardtii: a model for photosynthesis and so much more". In: *Nature Methods* (2023). DOI: https://doi.org/10.1038/s41592-023-02023-6.

[10] H. Eshgarf, A.A. Nadooshan, and A. Raisi. "An overview on properties and applications of magnetorheological fluids: Dampers, batteries, valves and brakes". In: *Journal of Energy Storage* (2022). DOI: https://doi.org/10.1016/j.est.2022.104648.

[11] I. Essafri et al. "Desiging, Synthetisizing, and modeling of active fluids". In: *AIP Publishing* (2022). DOI: https://doi.org/10.1063/5.0096955.

[12] A. Franck and M. Grehlinger. "Benefit of Fast Data Sampling during Rheological Testing". In: *TA Instruments, Inc.* (2004). URL: https://www.tainstruments.com/pdf/literature/L2083_Benefit_of_fast_data_sampling_for_rheological_testing.pdf.

[13] Z. Gao et al. "Using confined bacteria as building blocks to generate fluid flow". In: *Lab Chip* (2015). DOI: 10.1039/c5lc01093d.

[14] X. Gong et al. "Engineering reconfigurable flow patterns via surface-driven light-controlled active matter". In: *Physical Review Fluids* (2021). DOI: 10.1103/PhysRevFluids.6.123104.

[15] A.J. Hughes. "The Einstein Relation between Relative Viscosity and Volume Concentration of Suspensions of Spheres". In: *Nature* 173 (1954). DOI: https://doi.org/10.1038/1731089a0.

[16] A. Javadi et al. "Photo-bioconvection: towards light control of flows in active suspensions". In: *Phil. Trans. Royal Society A.* 378.2179 (2020). DOI: https://doi.org/10.1098/rsta.2019.0523.

[17] G.B. Jeffery. "The motion of ellipsoidal particles immersed in a viscous fluid". In: *Royal Society* 102.715 (1922). DOI: https://doi.org/10.1098/rspa.1922.0078.

[18] Azusa Kage et al. "Drastic reorganization of the bioconvection pattern of Chlamydomonas: quantitative analysis of the pattern transition response". In: *Journal of Experimental Biology* 216.24 (2013). DOI: https://doi.org/10.1242/jeb.092791.

[19] M.J. Kim and K. Breuer. "Microfluidic Pump Powered by Self-Organizing Bacteria". In: *Small* (2008). DOI: https://doi.org/10.1002/smll.200700641.

[20] M. Kojima et al. "Bacterial sheet-powered rotation of a micro-object". In: *Elsevier* (2015). DOI: https://doi.org/10.1016/j.snb.2015.07.071.

[21] N. Koumakis et al. "Targeted delivery of colloids by swimming bacteria". In: *Nature Communications* (2013). DOI: https://doi.org/10.1038/ncomms3588.

[22] Eric Lauga. *The Fluid Dynamics of Cell Motility*. Cambridge University Press, 2020. ISBN: 9781316626702.

[23] Eric Lauga and Sébastien Michelin. "Stresslets induced by active swimmers". In: *Physical Review Letters* 117.14 (2016). DOI: https://doi.org/10.1103/physrevlett.117.148001.

[24] M. Laun et al. "Guidelines for checking performance and verifying accuracy of rotational rheometers: viscosity measurements in steady and oscillatory shear (IUPAC Technical Report)". In: *Pure And Applied Chemistry* 86.12 (2014). DOI: https://doi.org/10.1515/pac-2013-0601.

[25] A. Lehmuskero, M.S. Chauton, and T. Boström. "Light and photosynthetic microalgae: A review of cellular- and molecular- scale optical processes". In: *Progress in Oceanography* (2018). DOI: https://doi.org/10.1016/j.pocean.2018.09.002.

[26] R. Di Leonardo et al. "Bacterial Ratchet Motors". In: *PNAS* (2010). DOI: https://doi.org/10.1073/pnas.0910426107.

[27] B. Maier. "How Physical Interactions Shape Bacterial Biofilms". In: *Annual Review of Biophysics* (2021). DOI: https://doi.org/10.1146/annurev-biophys-062920-063646.

[28] T. Majima and F. Oosawa. "Response of Chlamydomonas to Temperature Change". In: *The Journal of Protozoology* 22.4 (1975). DOI: https://doi.org/10.1111/j.1550-7408.1975.tb05218.x.

[29] Matthieu Martin et al. "Photofocusing: Light and flow of phototactic microswimmer suspension". In: *Physical review* 93.5 (2016). DOI: https://doi.org/10.1103/physreve.93.051101.

[30] Matthias Mussler et al. "Effective viscosity of non-gravitactic Chlamydomonas Reinhardtii microswimmer suspensions". In: *Europhysics Letters* 101.5 (2013). DOI: https://doi.org/10.1209/0295-5075/101/54004.

[31] Ueki N. et al. "Eyespot-dependent determination of the phototactic sign in Chlamydomonas Reinhardtii." In: *Proceedings of the National Academy of Sciences of the United States of America* 113.19 (2016). DOI: https://doi.org/10.1073/pnas.1525538113.

[32] T. O'Haver. *Signals and noise*. https://terpconnect.umd.edu/~toh/spectrum/SignalsAndNoise.html.

[33] A.G. Olabi and A. Grunwald. "Design and application of magneto-rheological fluid". In: *Materials in Engineering* 28.10 (2007). DOI: https://doi.org/10.1016/j.matdes.2006.10.009.

[34] Ewoldt R.H., Johnston M.T., and Caretta L. "Complex Fluids in Biological Systems". In: Springer, New York, NY, 2014. Chap. Experimental Challenges of Shear Rheology: How to Avoid Bad Data.

[35] Salima Rafai, Levan Jibuti, and Philippe Peyla. "Effective Viscosity of Microswimmer Suspensions". In: *Physical Review Letters* 104.9 (2010). DOI: https://doi.org/10.1103/physrevlett.104.098102.

[36] M. Rey, G. Volpe, and G. Volpe. "Light, Matter, Action: Shining Light on Active Matter". In: *ACS Photonics* (2023). DOI: https://doi.org/10.1021/acsphotonics.3c00140.

[37] Saintillan. "Rheology of active fluids". In: *Annual Review of Fluid Mechanics* 50.1 (2018). DOI: https://doi.org/10.1146/annurev-fluid-010816-060049.

[38] J. da Silva Pessoa et al. "Trends on Chlamydomonas reinhardtii growth regimes and bioproducts". In: *IUBMB Journals* (2023). DOI: https://doi.org/10.1002/bab.2486.

[39] A. Sokolov et al. "Swimming bacteria power microscopic gears". In: *Proc Natl Acad Sci U S A* (2010). DOI: 10.1073/pnas.0913015107.

[40] Andrey Sokolov and Igor Aranson. "Reduction of Viscosity in Suspension of Swimming Bacteria". In: *Physical Review Letters* 103.14 (2009). DOI: 10.1103/PhysRevLett.103.148101.

[41] Tullio Traverso. "Suspensions of active microparticles: collective dynamics and effective rheology of an active fluid". English. Fluid mechanics. Institut Polytechnique de Paris, 2021. fftel: 03486904 (physics.class-ph). URL: https://tel.archives-ouvertes.fr/tel-03486904.

[42] N. Ueki and K. Wakabayashi. "Phototaxis Assay for Chlamydomonas reinhardtii". In: *Bio-protocol* 7.12 (2017). DOI: https://doi.org/10.21769/bioprotoc.2356.

[43] *Water - Dynamic (Absolute) and Kinematic Viscosity vs. Temperature and Pressure*. https://www.engineeringtoolbox.com/water-dynamic-kinematic-viscosity-d_596.html.

[44] C. Rosie Williams and M.A. Bees. "A tale of three taxes: photo-gyro-gravitactic bioconvection". In: *Journal of Experimental Biology* 214.14 (2011). DOI: https://doi.org/10.1242/jeb.051094.

[45] Garcia X., Rafaï S., and Peyla P. "Light Control of the Flow of Phototactic Microswimmer Suspensions". In: *Physical Review Letters* 110.13 (2013). DOI: 10.1103/PhysRevLett.110.138106.

[46] Liu Z., Zhang K., and Cheng X. "Effective Viscosity of Microswimmer Suspensions". In: *Physical Review Letters* 58.8 (2019). DOI: https://doi.org/10.1007/s00397-019-01155-x.

[47] Yikai Zhao. "Motility of Chlamydomonas reinhardtii at different temperatures". In: *TU Delft* (2023). URL: http://repository.tudelft.nl/.

Appendix A

Culture Scheme

The scheme shows a step-by-step guide for culturing the green algae.

Turn on air filtering machine by pressing ON and turn on the lights. Wait until all lights are green. Do not modify other options. This machine absorbs air from above, filters the air in order to work in a clean environment and blows the clean air into the working space before sucking the air back out. The machine can be opened on two heights only (closed and middle).
Clean the working surface with product and clean paper.
Equipment: • Test tube of previous mother culture of Chlamydomonas reinhardtii CC125 • Erlenmeyer clean and decontaminated (Visible by a cotton with an aluminium film on top) • Air tube (same amount as Erlenmeyer) • TAP medium • Loop (same amount as Erlenmeyer) • Filter (same amount as Erlenmeyer) (Filters are always on the left of the working surface) • 1 Parafilm Prepare the supplies in advance by placing them on the left of the working surface. This is to reduce risk of contamination. Used, contaminated supplies will be placed on the right of the working surface.
Wash hands and place hands at least 10 cm into the work space. Do not cross hands throughout the entire lab.
Remove aluminium foil and cotton from the Erlenmeyer. Do not destroy them as they will be used later again. Place them upside down on the working surface with the cotton onto the aluminium foil. Pour 300 ml of TAP medium into the Erlenmeyer.
Take the test tube containing the algae in left hand and open it by removing the parafilm. Use the blue loop to extract the algae (dark green part) with your right hand. Do not touch the side walls of the test tube while inserting and removing the loop. Than take the Erlenmeyer with your left hand and insert the blue loop until you reach the medium. Stir the loop in the medium in order to diffuse the algae extraction. Place the blue loop to the right of the working surface.
Place the air tube into the Erlenmeyer using a tweezer. Close the Erlenmeyer with the cotton and the aluminium film. Connect the filter with the air tube. Repeat the 3 previous steps according to the number of Erlenmeyer flasks used.
Use the new parafilm to close the test tube of the previous mother culture. On the aluminium film of the Erlenmeyer, write down name initials, strain of C. reinhardtii (CC125), medium (TAP) and two dates below (S1 and S2). The dates are as following: S1 = date of the previous mother culture(which is equal to S2 on the test tube), S2 = date of the current culture.
Place the Erlenmeyer flasks into the refrigerator. Connect the air tube of the refrigerator with the filter on the air tube of the Erlenmeyer flask. Adjust the air mass flow by turning the blue wheel until approximately 1 bubble per second is achieved.
Throw away all used utensils and place the mother culture back into the light-dark cycle box. Clean the working surface with product and paper. Turn off the machine. Check cultures again within 2 hours to check the air mass flow.

Figure A.1: Step-by-step scheme for making a culture of the *Chlamydomonas reinhardtii*.

Appendix B

Light Refraction

This appendix shows how the tilt angle of the light controlling design was achieved.

$$n_1 \sin\theta_1 = n_2 \sin\theta_2 = n_3 \sin\theta_3 \tag{B.1}$$

The equation includes the refractive indices of the medium through which a light beam travels. The light travels through air (1), glass (2) and water (3), which have a refractive index of $n_1 = 1$, $n_2 = 1.51$ and $n_3 = 1.33$ respectively. It is worth highlighting that the light actually travels through the active fluid suspension and not through pure water. According to literature, the body cells of the algae have a refractive index slightly higher than water and lies between 1.39 and 1.51 [25]. The suspensions are diluted in water, and because their body consists for the biggest part of water, the active fluid suspension has a refractive index close to water. Therefore the refraction index of water was taken for the active fluid medium.

The orientation axis of the algae is at a 45° angle with the vertical axis and therefore the light should penetrate at this angle $\theta_3 = 45°$. In order to find the tilt angle required for the light guiding structure, the equation above is used to calculate the light refraction.

$$\theta_1 = \arcsin\frac{n_3 \sin\theta_3}{n_1} = \arcsin\frac{1.33 \cdot \sin 45°}{1} \tag{B.2}$$

This results in the angle $\theta_2 = 70°$.

Additionally, it is verified that no total internal reflection occurs. This condition is effective when the angle of incident is greater than the critical angle. The relationship is as following, with the critical angle, the term on the right-hand side:

$$\theta_1 > \arcsin\frac{n_2}{n_1} \tag{B.3}$$

for $n_1 > n_2$. The total internal reflection can occur only at the bottom boundary of the glass. At this boundary, the respective angle of incidence is $\theta_2 = 38.4°$, calculating it through equation B.1, whereas the critical angle for total internal reflection occurs at $\theta_c = 61.7°$. This means that total internal reflection can be disregarded.

Appendix C

Figures of Tubes

The appendix shows the design of the tubes which guide the light to the sample with algae suspensions on the rheometer. The circular structure forms half a circle for the ease of positioning the tubes in the frame around the shaft of the rheometer during experimentation. This structure is 3D printed. The tubes are tilted at 70° with the vertical axis. Two types were designed for the experiments. One is designed for the LED strip and the other for the blue LED Phlatlight. The blue LED Phlatlight has fewer tubes, because of the amount of place available to place the lights. Each tube also consists of a support for the lights.

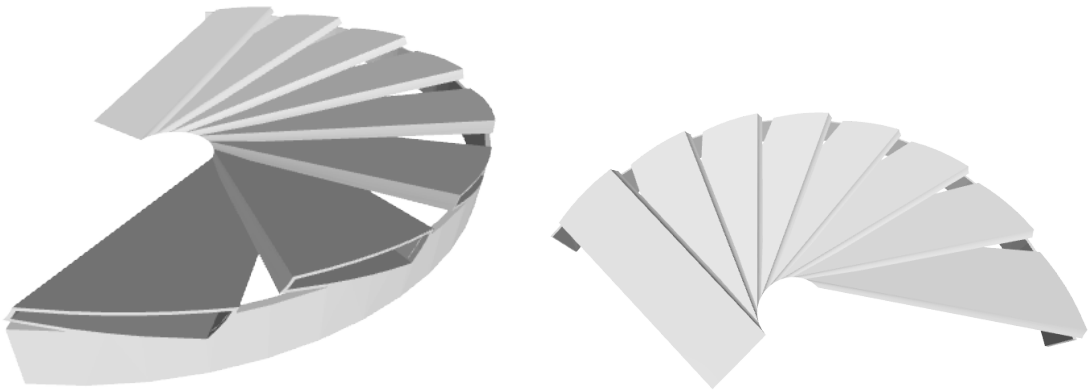

(a) Side view (b) Top view

Figure C.1: Structure op tubes in a circular pattern are tilted at 70° with the vertical axis.

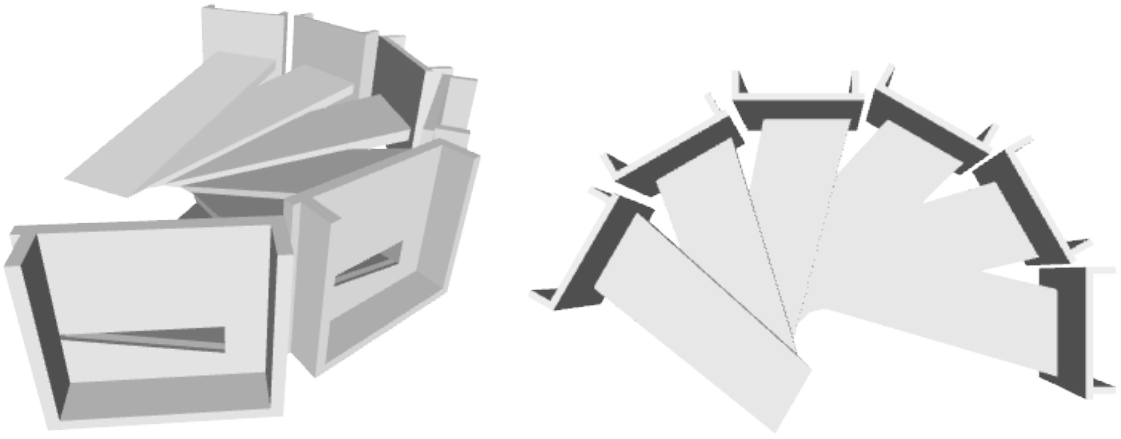

(a) Side view (b) Top view

Figure C.2: Structure op tubes for LED Phlatlight in a circular pattern are tilted at 70° with the vertical axis.

Appendix D

Data of Positif Shear Rate Rheology Measurements

D.1 Shear Rate $1\,s^{-1}$

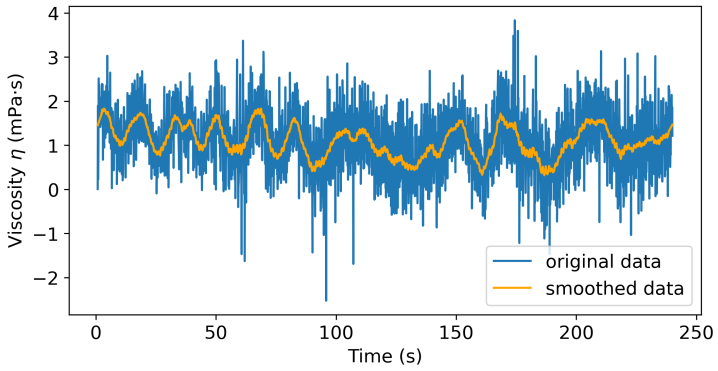

(a) Time-domain for dark suspensions

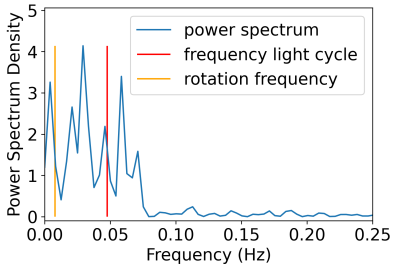

(b) Power spectrum dark

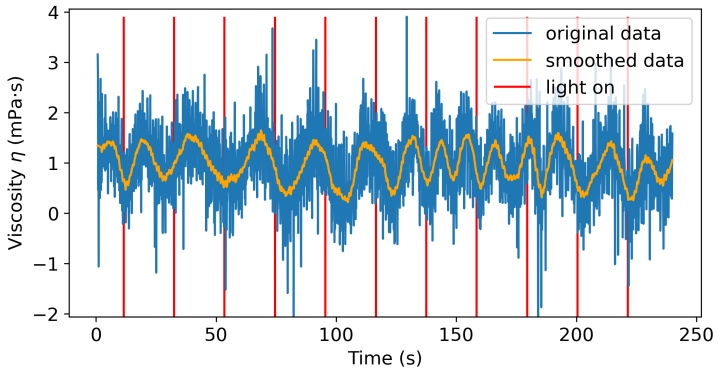

(c) Time-domain for light-controlled suspensions

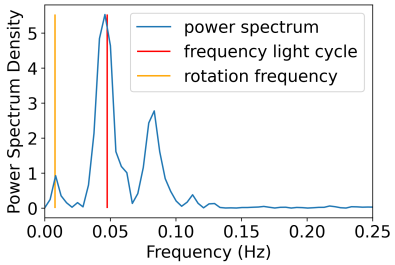

(d) Power spectrum light-control

Figure D.1: 0.5% algal sample at a shear rate of $1\,s^{-1}$. Noise power amplitude for the dark algae is 0.35 and for the light-controlled algae is 0.35.

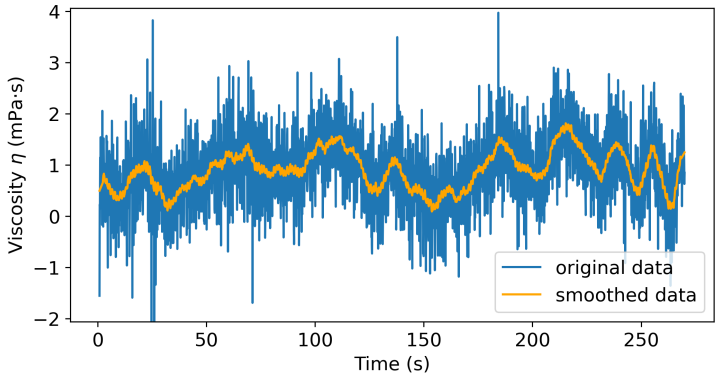

(a) Time-domain for dark suspensions

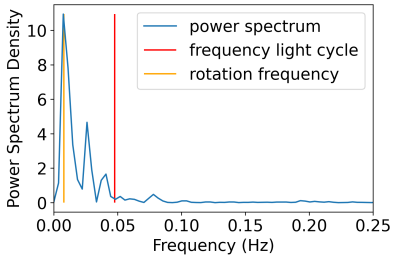

(b) Power spectrum dark

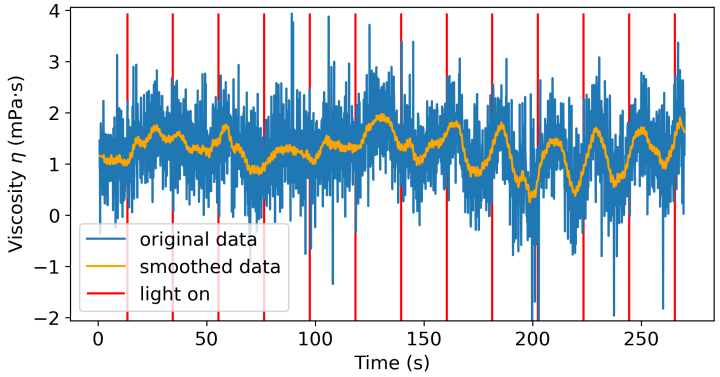

(c) Time-domain for light-controlled suspensions

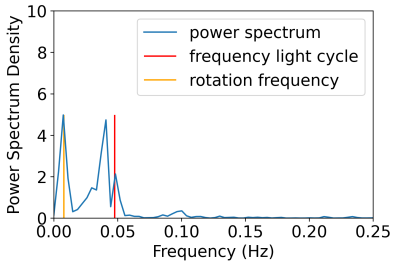

(d) Power spectrum light-control

Figure D.2: 1% algal sample at a shear rate of $1\,s^{-1}$. Noise power amplitude for the dark algae is 0.45 and for the light-controlled algae is 0.35.

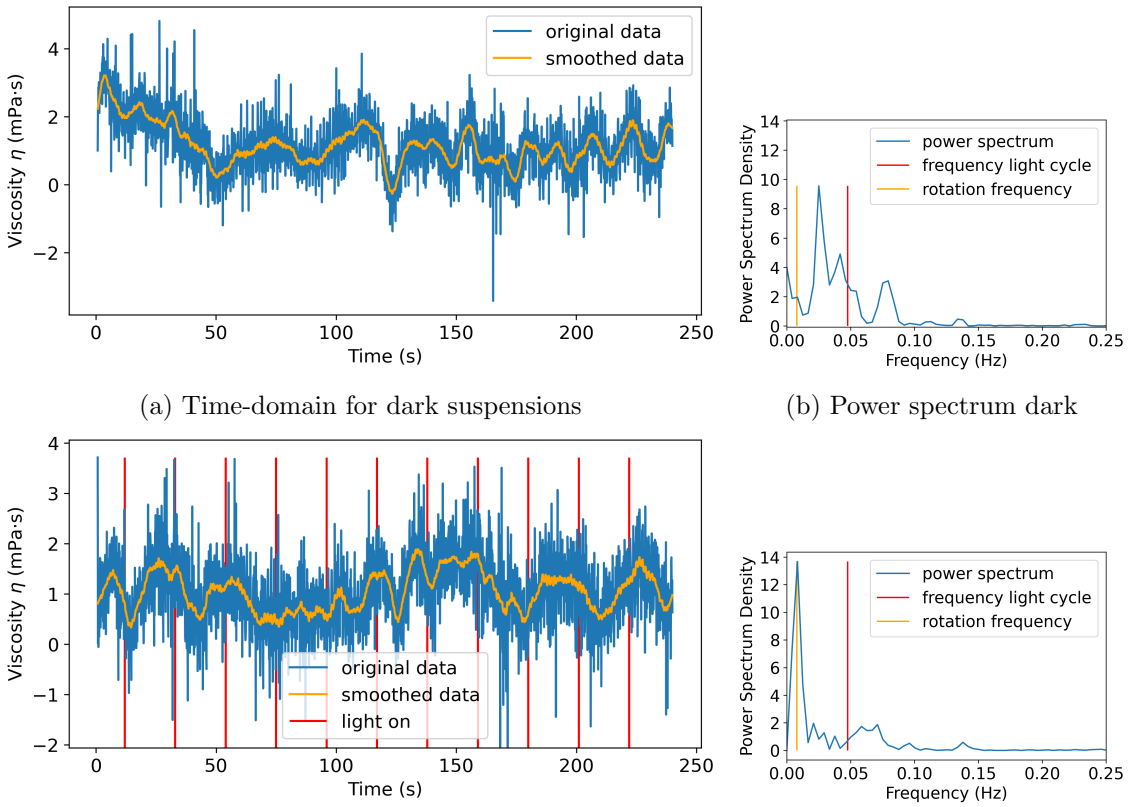

(a) Time-domain for dark suspensions

(b) Power spectrum dark

(c) Time-domain for light-controlled suspensions

(d) Power spectrum light-control

Figure D.3: 2% algal sample at a shear rate of $1\,s^{-1}$. Noise power amplitude for the dark algae is 0.35 and for the light-controlled algae is 0.1.

D.2 Shear Rate $4\,s^{-1}$

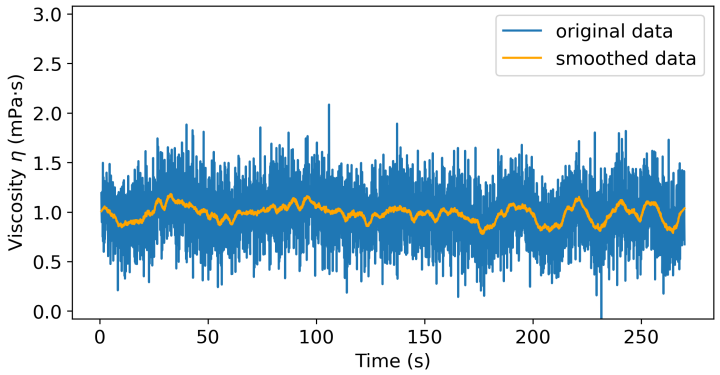

(a) Time-domain for dark suspensions

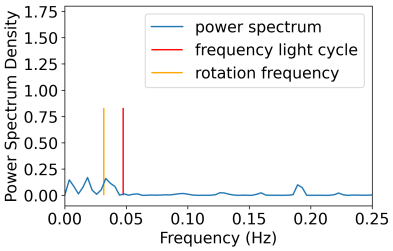

(b) Power spectrum dark

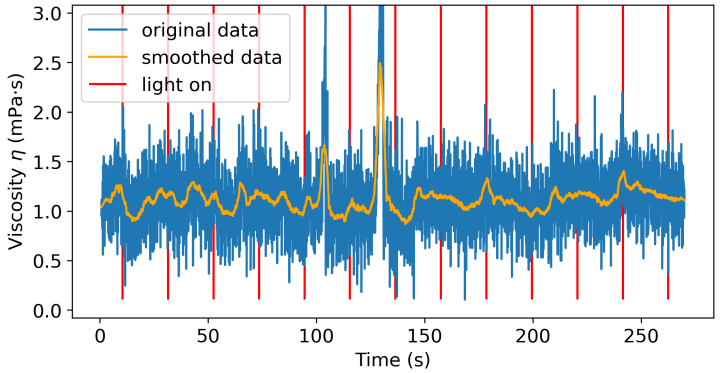

(c) Time-domain for light-controlled suspensions

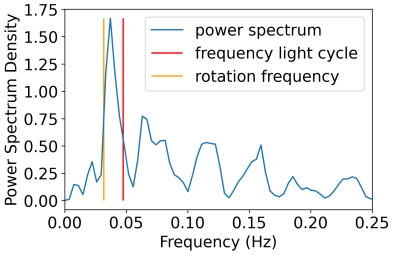

(d) Power spectrum light-control

Figure D.4: 1% algal sample at a shear rate of $4\,s^{-1}$. Noise power amplitude for the dark algae is 0.08 and for the light-controlled algae is 0.05.

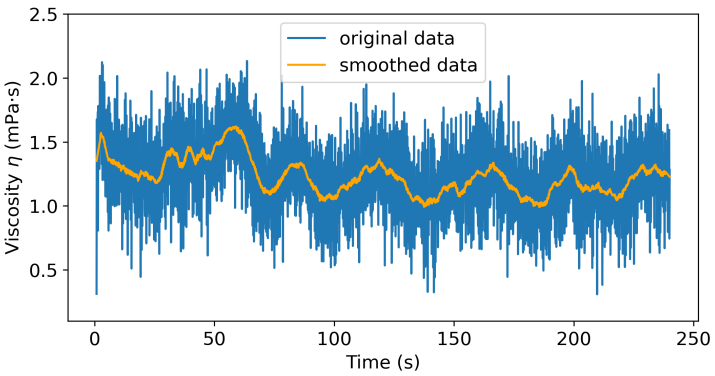

(a) Time-domain for dark suspensions

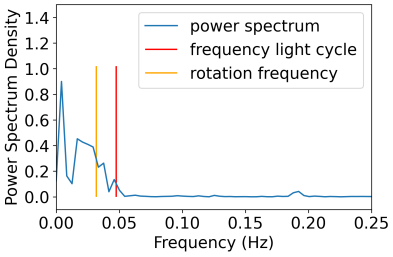

(b) Power spectrum dark

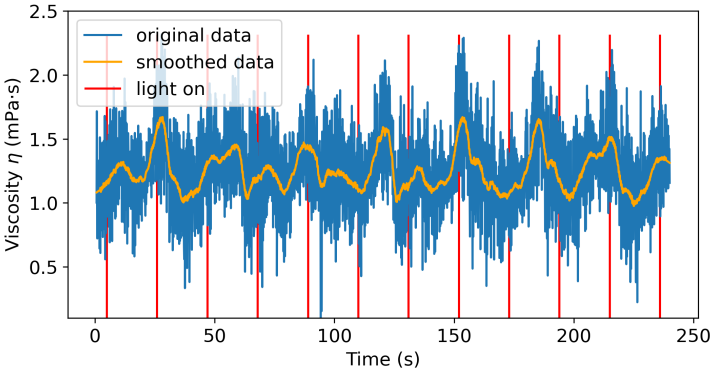

(c) Time-domain for light-controlled suspensions

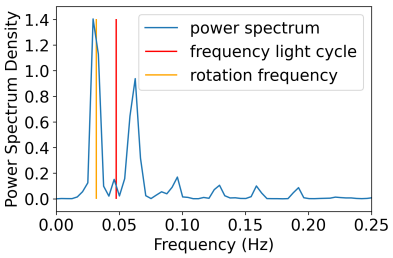

(d) Power spectrum light-control

Figure D.5: 2% algal sample at a shear rate of $4\,s^{-1}$. Noise power amplitude for the dark algae is 0.03 and for the light-controlled algae is 0.08.

D.3 Shear Rate $10\,s^{-1}$

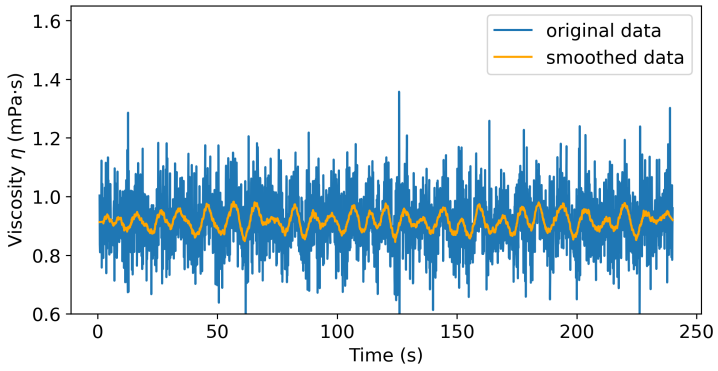

(a) Time-domain for dark suspensions

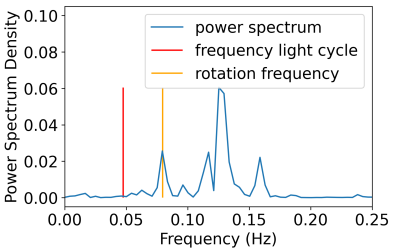

(b) Power spectrum dark

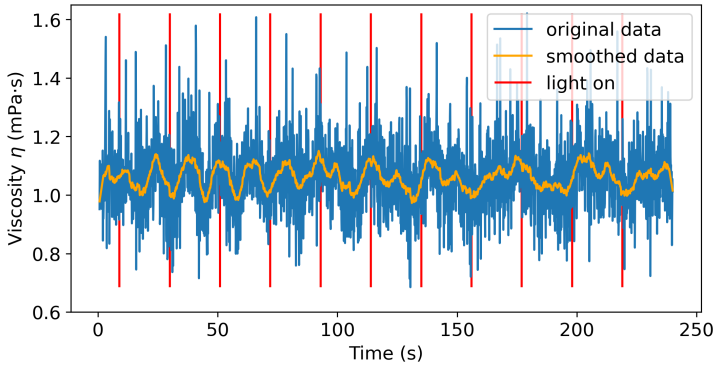

(c) Time-domain for light-controlled suspensions

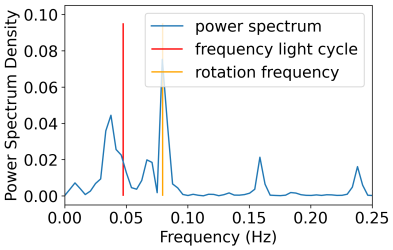

(d) Power spectrum light-control

Figure D.6: 0.5% algal sample at a shear rate of $10\,s^{-1}$. Noise power amplitude for the dark algae is 0.01 and for the light-controlled algae is 0.01.

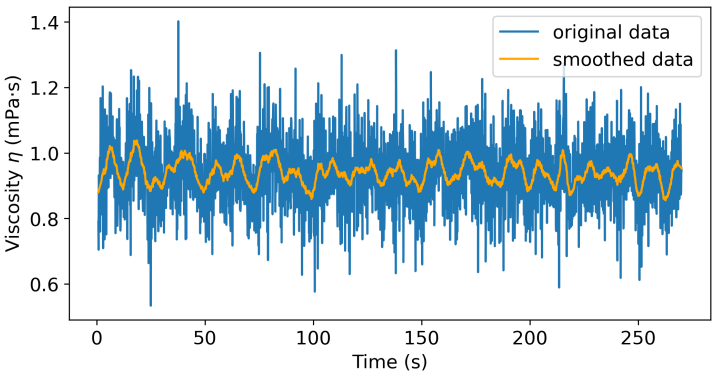

(a) Time-domain for dark suspensions

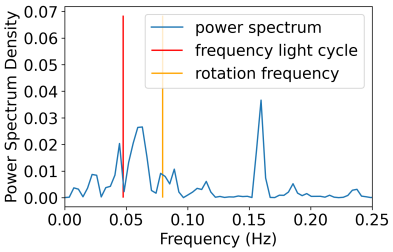

(b) Power spectrum dark

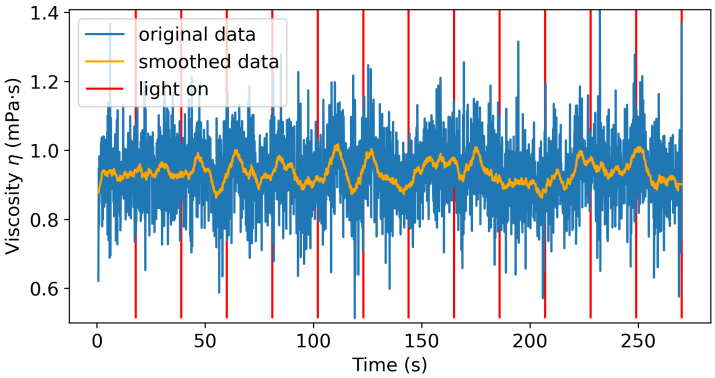

(c) Time-domain for light-controlled suspensions

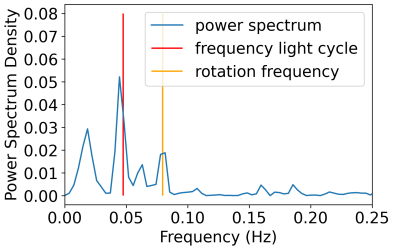

(d) Power spectrum light-control

Figure D.7: 1% algal sample at a shear rate of $10\,s^{-1}$. Noise power amplitude for the dark algae is 0.01 and for the light-controlled algae is 0.006.

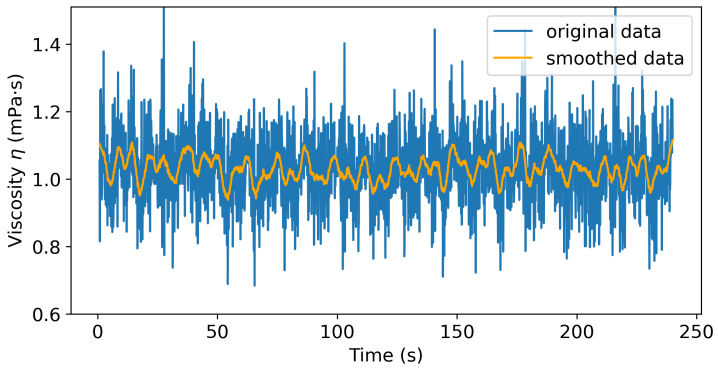

(a) Time-domain for dark suspensions

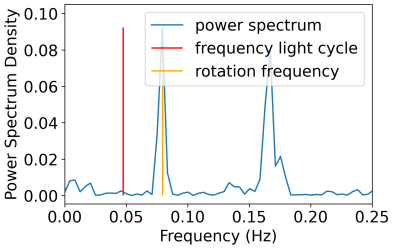

(b) Power spectrum dark

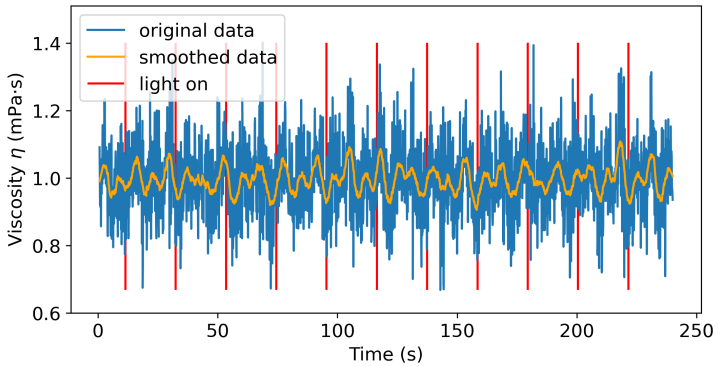

(c) Time-domain for light-controlled suspensions

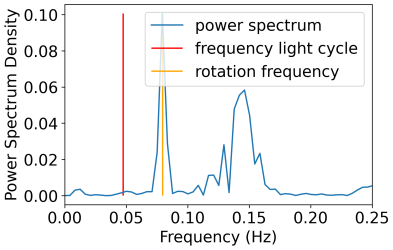

(d) Power spectrum light-control

Figure D.8: 2% algal sample at a shear rate of $10\,s^{-1}$. Noise power amplitude for the dark algae is 0.01 and for the light-controlled algae is 0.01.

Appendix E

Data of Inversed Shear Rates

E.1 Shear Rate $-1\,s^{-1}$

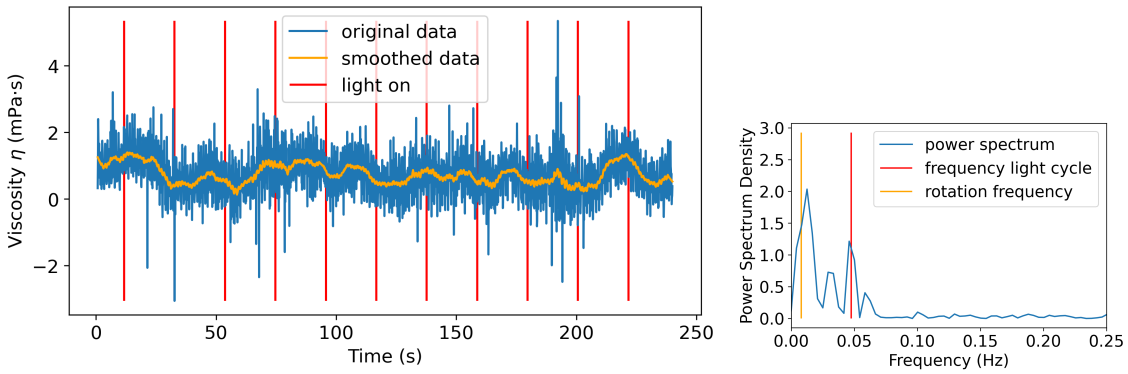

(a) Time-domain signal (b) Power spectrum

Figure E.1: signal of viscosity of 0.5% algae under light-control at shear rate of $-1\,s^{-1}$

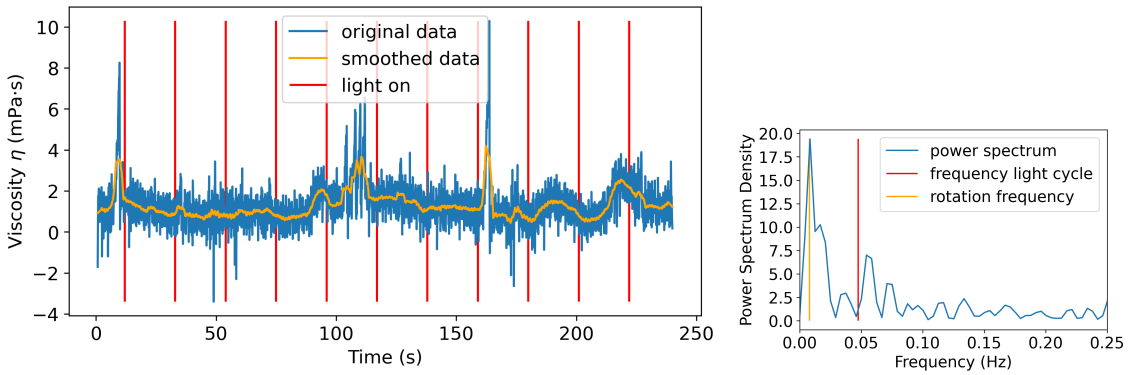

(a) Time-domain signal (b) Power spectrum

Figure E.2: signal of viscosity of 1% algae under light-control at shear rate of $-1\,s^{-1}$

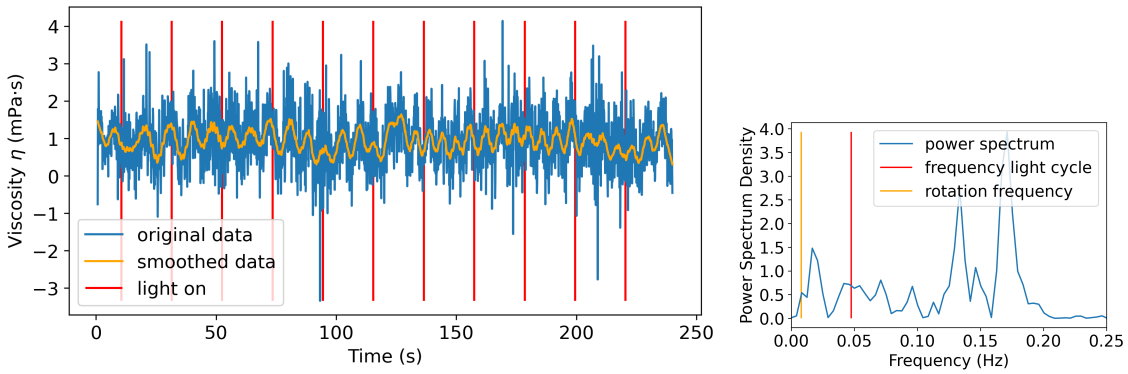

(a) Time-domain signal (b) Power spectrum

Figure E.3: signal of viscosity of 2% algae under light-control at shear rate of $-1\,s^{-1}$

E.2 Shear Rate $-4\,s^{-1}$

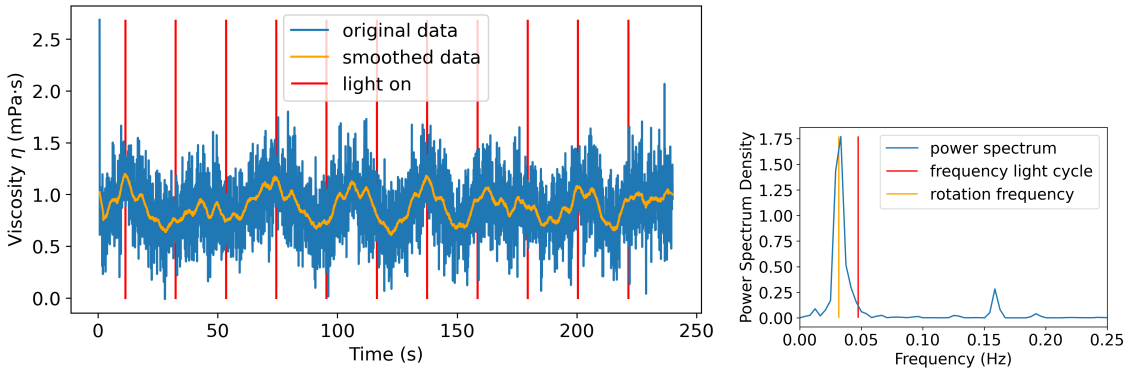

(a) Time-domain signal (b) Power spectrum

Figure E.4: signal of viscosity of 0.5% algae under light-control at shear rate of $-4\,s^{-1}$

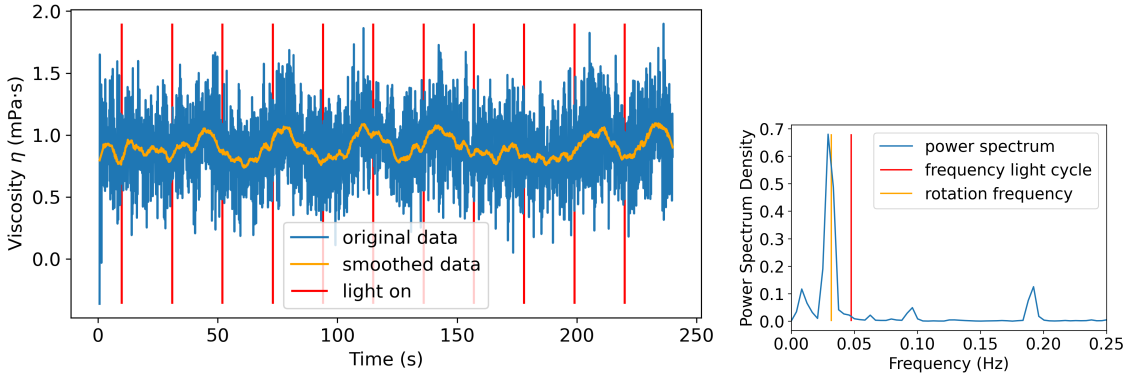

(a) Time-domain signal (b) Power spectrum

Figure E.5: signal of viscosity of 1% algae under light-control at shear rate of $-4\,s^{-1}$

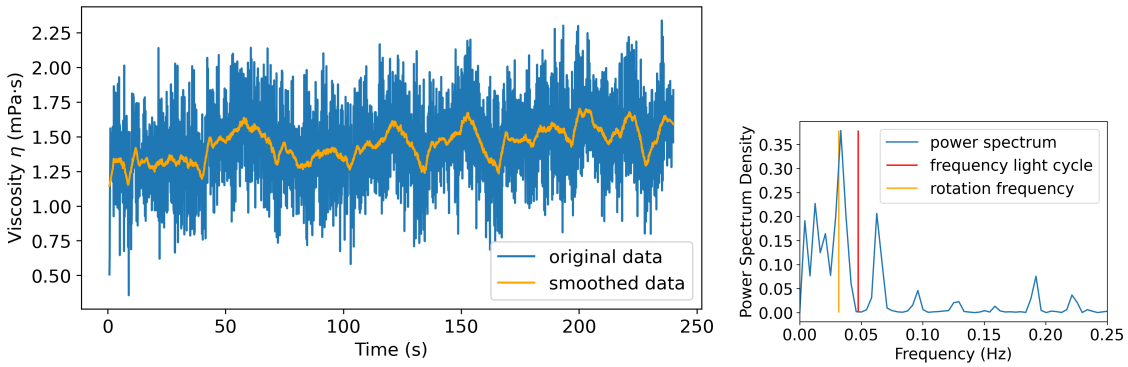

(a) Time-domain signal (b) Power spectrum

Figure E.6: signal of viscosity of 2% algae under light-control at shear rate of $-4\,s^{-1}$

E.3 Shear Rate $-10\,s^{-1}$

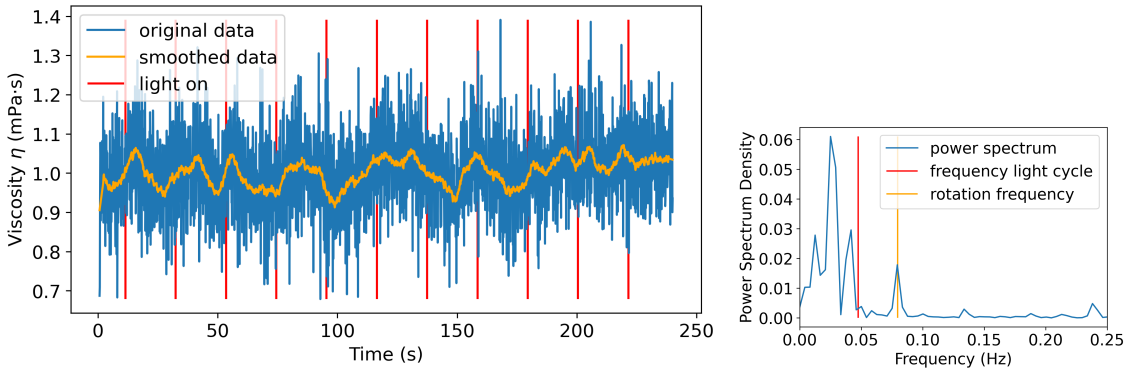

(a) Time-domain signal (b) Power spectrum

Figure E.7: signal of viscosity of 0.5% algae under light-control at shear rate of $-10\,s^{-1}$

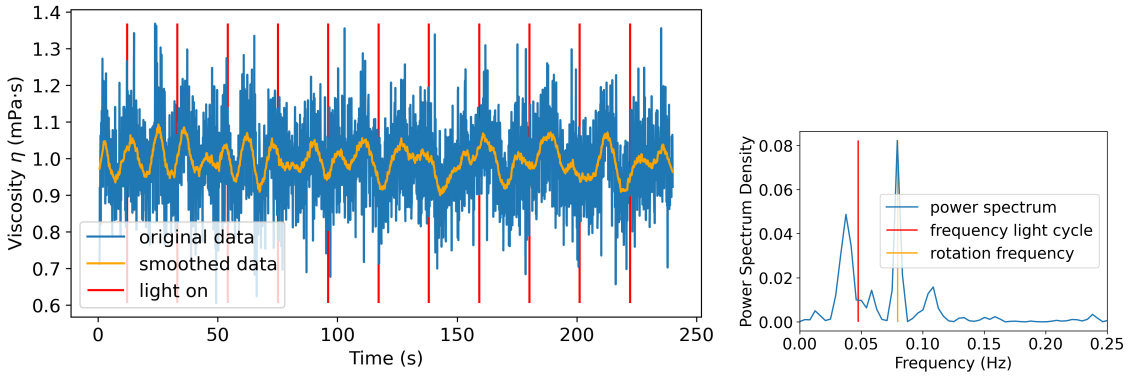

(a) Time-domain signal (b) Power spectrum

Figure E.8: signal of viscosity of 1% algae under light-control at shear rate of $-10\,s^{-1}$

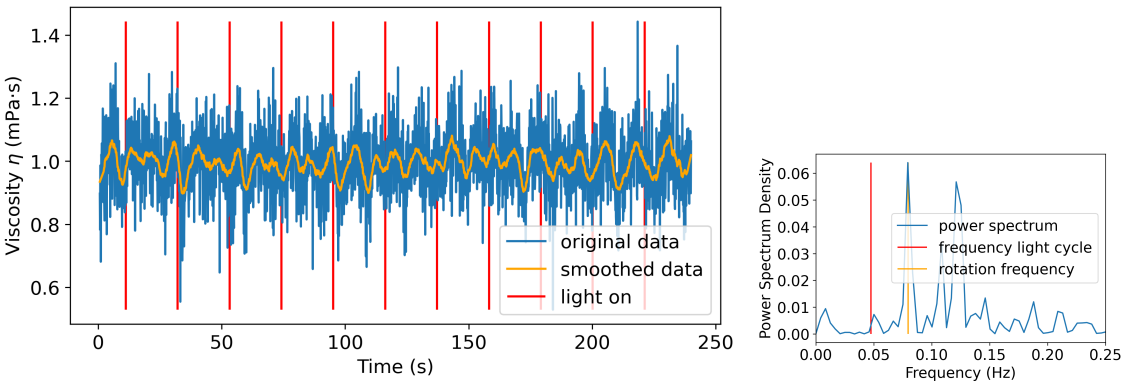

(a) Time-domain signal

(b) Power spectrum

Figure E.9: signal of viscosity of 2% algae under light-control at shear rate of $-10\,s^{-1}$

Appendix F

Data of Dead and Live Algae

The data represent the difference between dead and active organisms. The viscosity is normalized by the suspending medium, which is TAP for live algae and a mixture of TAP and Betadine for dead algae.

F.1 Shear Rate $1\,s^{-1}$

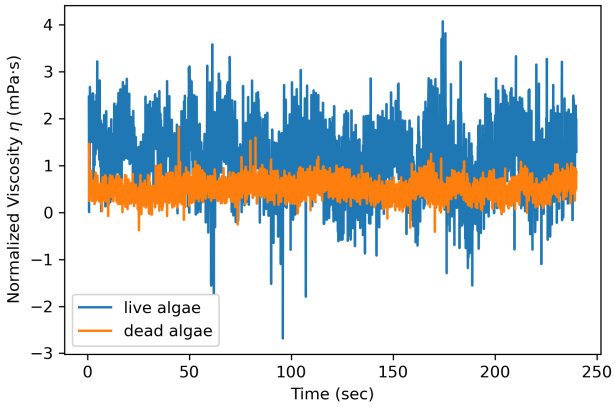

Figure F.1: Difference in dynamic viscosity between 0.5% dead and live algae at a shear rate of $1\,s^{-1}$

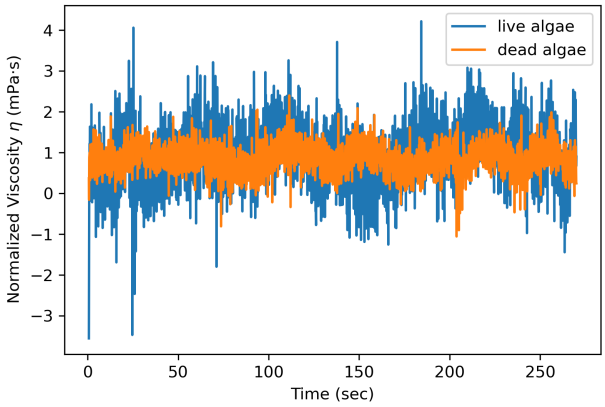

Figure F.2: Difference in dynamic viscosity between 1% dead and live algae at a shear rate of $1\,s^{-1}$

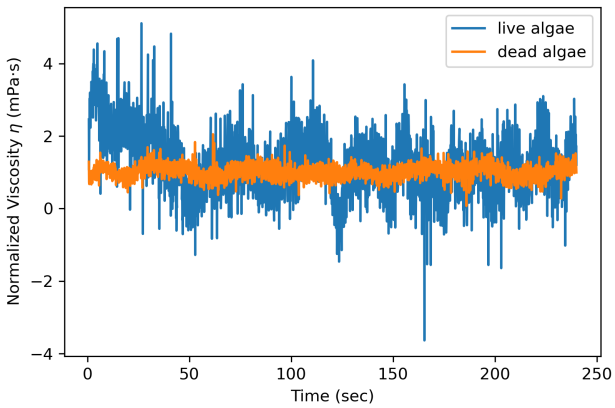

Figure F.3: Difference in dynamic viscosity between 2% dead and live algae at a shear rate of $1\,s^{-1}$

F.2 Shear Rate $4\,s^{-1}$

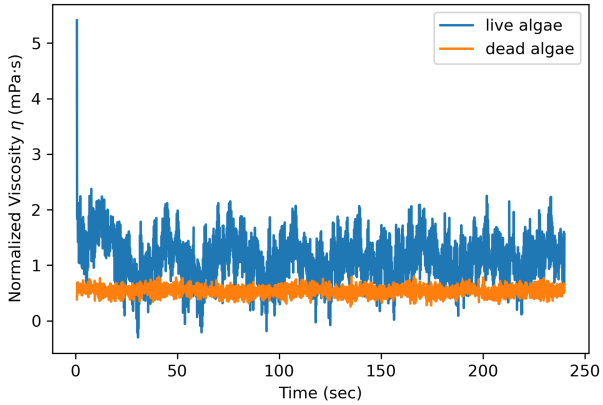

Figure F.4: Difference in dynamic viscosity between 0.5% dead and live algae at a shear rate of $4\,s^{-1}$

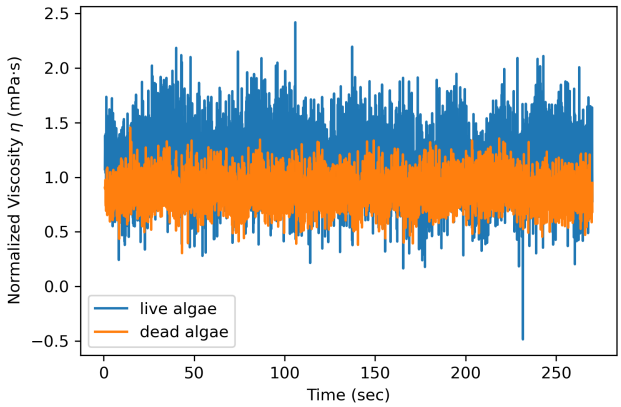

Figure F.5: Difference in dynamic viscosity between 1% dead and live algae at a shear rate of $4\,s^{-1}$

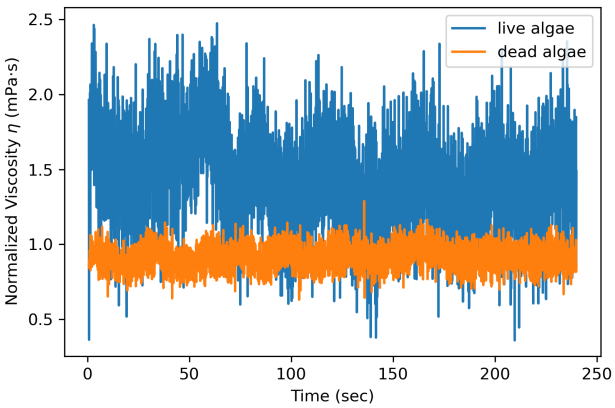

Figure F.6: Difference in dynamic viscosity between 2% dead and live algae at a shear rate of $4\,s^{-1}$

F.3 Shear Rate $10\,s^{-1}$

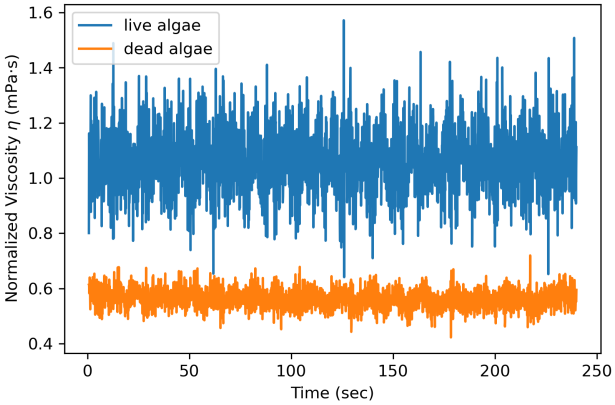

Figure F.7: Difference in dynamic viscosity between 0.5% dead and live algae at a shear rate of $10\,s^{-1}$

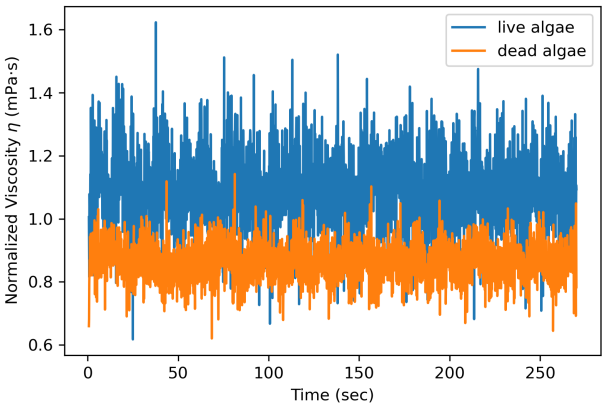

Figure F.8: Difference in dynamic viscosity between 1% dead and live algae at a shear rate of $10\,s^{-1}$

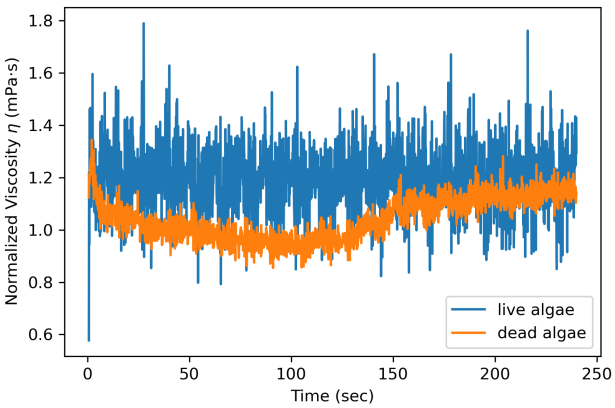

Figure F.9: Difference in dynamic viscosity between 2% dead and live algae at a shear rate of $10\,s^{-1}$

Appendix G

Data of 6% Volume Fraction

During the thesis, multiple experimental trials were done including higher shear rates and higher volume fractions. To remain in the low shear methodology, shear rates of 1 and $4\,s^{-1}$ are shown for the 6% volume fraction of *Chlamydomonas reinhardtii* suspensions. A considerable increase is found in the power spectrum at the light-cycle frequency, indicating a stress response to the reorientation of the algae.

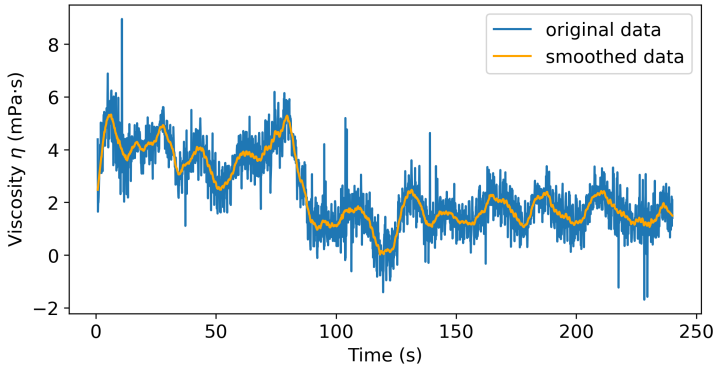

(a) Time-domain signal

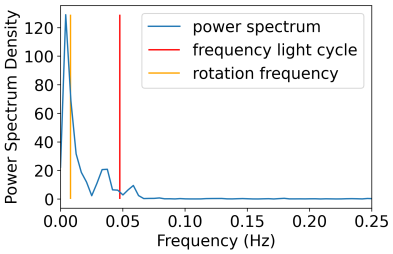

(b) Power spectrum dark

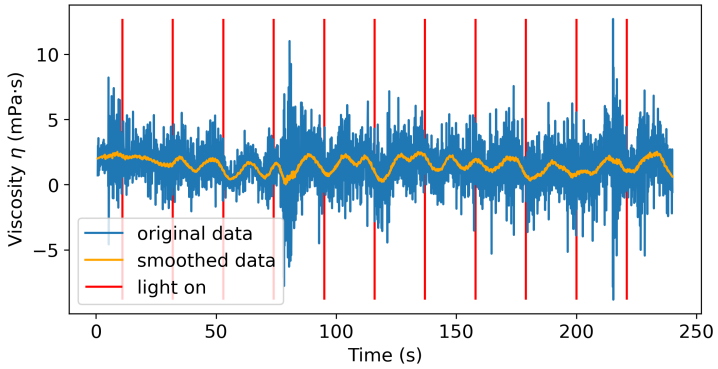

(c) Time-domain for light-controlled suspensions

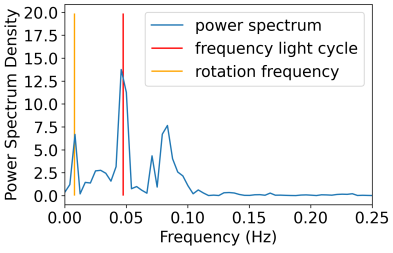

(d) Power spectrum light-control

Figure G.1: 6% algal sample at a shear rate of $1\,s^{-1}$.

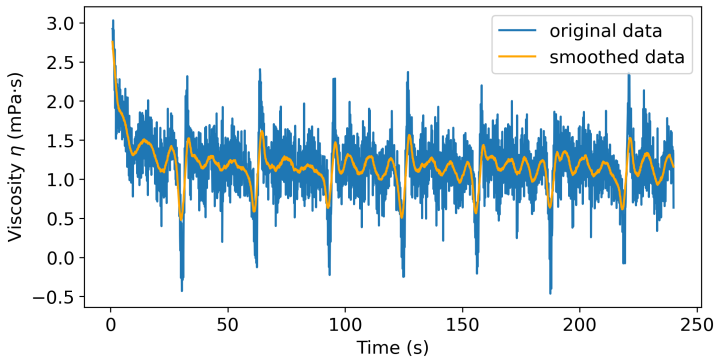

(a) Time-domain signal

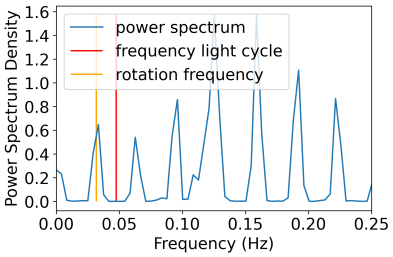

(b) Power spectrum dark

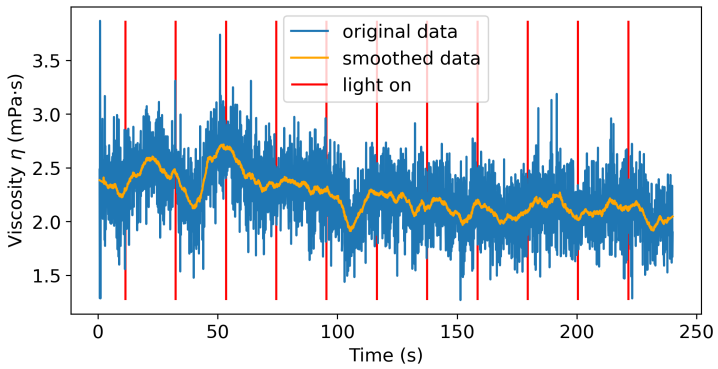

(c) Time-domain for light-controlled suspensions

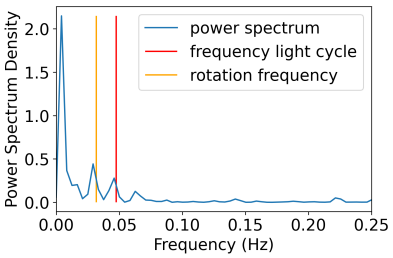

(d) Power spectrum light-control

Figure G.2: 6% algal sample at a shear rate of $4\,s^{-1}$.